

Chemical speciation models based upon the Pitzer activity coefficient equations, including the propagation of uncertainties: Artificial seawater from 0 to 45 °C

Matthew P. Humphreys^{a,b}, Jason F. Waters^c, David R. Turner^d, Andrew G. Dickson^e, Simon L. Clegg^{a,*}

^a School of Environmental Sciences, University of East Anglia, Norwich NR4 7TJ, United Kingdom

^b NIOZ Royal Netherlands Institute for Sea Research, Department of Ocean Systems (OCS), P.O. Box 59, 1790 AB Den Burg, Texel, Netherlands

^c National Institute of Standards and Technology, Gaithersburg, MD 20899, USA

^d Department of Marine Sciences, University of Gothenburg, Box 461, SE-40530 Gothenburg, Sweden

^e University of California at San Diego, Scripps Institution of Oceanography, 9500 Gilman Drive, La Jolla, CA 92093, USA

ARTICLE INFO

Keywords:

Seawater

Chemical speciation

Activity coefficient

pH

ABSTRACT

Accurate chemical speciation models of solutions containing the ions of seawater have applications in the calculation of carbonate system equilibria and trace metal speciation in natural waters, and the determination of pH. Existing models, based on the Pitzer formalism for the calculation of activity coefficients, do not yet agree with key experimental data (potentiometric determinations of H^+ and Cl^- activity products in acidified artificial seawaters) and, critically, do not include uncertainty estimates. This hampers applications of the models, and also their further development (for which the uncertainty contributions of individual ion interactions and equilibrium constants need to be known). We have therefore implemented the models of Waters and Millero (Mar. Chem. 149, 8–22, 2013) and Clegg and Whitfield (Geochim. et Cosmochim. Acta 59, 2403–2421, 1995) for artificial seawater, within a generalised treatment of uncertainties, as a first step towards a more complete model of standard seawater and pH buffers. This addition to the models enables both the total uncertainty of any model-calculated quantity (e.g., pH, speciation) to be estimated, and also the contributions of all interaction parameters and equilibrium constants. Both models have been fully documented (and some corrections made). Estimates of the variances and covariances of the interaction parameters were obtained by Monte Carlo simulation, with simplifying assumptions. The models were tested against measured electromotive forces (EMFs) of cells containing acidified artificial seawaters. The mean offsets (measured – calculated) at 25 °C for the model of Waters and Millero are: 0.046 ± 0.11 mV (artificial seawater without sulphate, $0.280 \text{ mol kg}^{-1}$ to $0.879 \text{ mol kg}^{-1}$ ionic strength); and -0.199 ± 0.070 mV (artificial seawater, salinities 5 to 45). Results are similar at other temperatures. These differences compare with an overall uncertainty in the measured EMFs of about 0.04 mV. Total uncertainties for calculated EMFs of the solutions were dominated by just a few contributions: mainly H^+-Cl^- , Na^+-Cl^- , and $H^+-Na^+-Cl^-$ ionic interactions, and the thermodynamic dissociation constant of HSO_4^- . This makes it likely that the accuracy of the models can readily be improved, and recommendations for further work are made. It is shown that standard EMFs used in the calibration of the marine ‘total’ pH scale can be accurately predicted with only slight modification to the original models, suggesting that they can contribute to the extension of the scale to lower salinities.

1. Introduction

Artificial seawater contains the major ions Na^+ , Mg^{2+} , Ca^{2+} , K^+ , Cl^- and SO_4^{2-} (with H^+ , HSO_4^- , OH^- and $MgOH^+$ included as minor species

for the purposes of acid-base calculations), and chemical speciation models using the Pitzer equations for activity coefficients have been developed for solutions containing these ions over a range of temperatures (Campbell et al., 1993; Clegg and Whitfield, 1995; Waters and Millero, 2013). Such models form the main element of larger models of

* Corresponding author.

E-mail address: s.clegg@uea.ac.uk (S.L. Clegg).

<https://doi.org/10.1016/j.marchem.2022.104095>

Received 16 August 2021; Received in revised form 2 February 2022; Accepted 3 February 2022

Available online 12 February 2022

0304-4203/© 2022 The Authors. Published by Elsevier B.V. This is an open access article under the CC BY license (<http://creativecommons.org/licenses/by/4.0/>).

Glossary of symbols*Pitzer interaction parameters*

$\beta_{ca}^{(0)}$, $\beta_{ca}^{(1)}$, $\beta_{ca}^{(2)}$, $C_{ca}^{(0)}$, $C_{ca}^{(1)}$ For interactions between cation c and anion a. Not all of these may be used, e.g., $\beta_{ca}^{(2)}$ is usually for 2:2 charge types only (e.g., CaSO_4), and is set to zero otherwise.

α_{ca} , $\alpha_{ca}^{(2)}$, ω_{ca} Coefficients associated with the ionic strength terms in the functions that use parameters $\beta_{ca}^{(1)}$, $\beta_{ca}^{(2)}$, and $C_{ca}^{(1)}$, respectively.

$\theta_{cc'}$, $\theta_{aa'}$ For interactions between dissimilar cations c and c', and between dissimilar anions a and a', respectively.

$\Psi_{cc'a}$, $\Psi_{aa'c}$ For interactions between anion a and dissimilar cations c and c', and between cation c and dissimilar anions a and a', respectively.

λ_{nc} , λ_{na} For interactions between neutral solute n and cation c, and between neutral solute n and anion a, respectively.

λ_{nn} , μ_{nnn} For the self-interaction of neutral solute n.

ζ_{nca} For the interaction between neutral solute n, cation c and anion a.

Other symbols used in the text

a_X Activity (molality basis) of species X, equivalent to $m_X \cdot \gamma_X$ where γ_X is the activity coefficient of X.

$\Delta_r C_p^\circ$ Heat capacity change for a reaction at constant pressure ($\text{J mol}^{-1} \text{K}^{-1}$).

D Coefficient by which the systematic error parameters $\Delta\phi_{\text{sys}}(i)$ are multiplied to obtain the contributions to the simulated osmotic coefficients in a dataset. See Eq. (4), and the explanation that follows.

E Electrode potential (V) in a Harned cell.

E^0 Standard electrode potential (V) of a Harned cell.

$\Delta(E - E^0)$ The difference between model-calculated and measured values of $(E - E^0)$, see definitions above and Eq. (6).

E^* The standard potential (V), on a total H^+ basis, defined by Eq. (13). It is obtained empirically by extrapolating Harned cell potentials to zero HCl molality in an artificial seawater of a specified composition and temperature (Eq. (14)), and can also be calculated directly using speciation models.

E' The left hand side of Eq. (14) (plotted in Fig. 13), which is equivalent to E^* in the limit of zero added HCl.

F The Faraday constant ($96,485.33212 \text{ C mol}^{-1}$).

$H(i)$ Coefficient by which the random error parameter $\Delta\phi_{\text{rdm}}(i)$ is multiplied to obtain the contribution to each simulated osmotic coefficient in a dataset. See Eq. (5), and the explanation that follows.

I Ionic strength, on a molality basis ($0.5 \sum_i m_i |z_i|^2$, where z_i is the charge on ion i and the summation is over all ions).

K Thermodynamic equilibrium constant (molality basis), expressing the relationship between the quotient of the activities of the product(s) and reactants(s) It is a function of temperature and pressure. Example: $K(\text{HSO}_4^-) = a\text{H}^+ \cdot a\text{SO}_4^{2-} / a\text{HSO}_4^-$, where a denotes activity.

K^* Stoichiometric equilibrium constant (on a molality basis), expressing the relationship between the quotient of the molalities of the product(s) and reactants(s) It varies with temperature, pressure, and solution composition. Example: $K^*(\text{HSO}_4^-) = m\text{H}^+ \cdot m\text{SO}_4^{2-} / m\text{HSO}_4^- = K(\text{HSO}_4^-) \cdot \gamma_{\text{HSO}_4^-} / (\gamma_{\text{H}^+} \cdot \gamma_{\text{SO}_4^{2-}})$.

$K^*(\text{HSO}_4^-)^{(\text{tr})}$ 'Trace' value of the stoichiometric bisulphate dissociation constant in artificial seawater, which is its value in the limit of zero added HCl (i.e., for a composition of pure artificial seawater at some specified salinity and temperature).

m_X Molality of species X (moles per kg of pure water solvent, with the units ' mol kg^{-1} ').

$m\text{SO}_4^{2-(\text{T})}$ Total molality of sulphate in an aqueous solution.

pH_T The pH on the total scale (expressed on a moles per kg of solution basis), defined by Dickson (1990) and DelValls and Dickson (1998).

pX The vapour pressure of species X.

p_{atm} Atmospheric pressure.

R The gas constant ($8.31446 \text{ J mol}^{-1} \text{K}^{-1}$)

S Salinity. Strictly, this definition refers to seawater only and for the artificial seawaters considered in this work S is a nominal salinity.

T Temperature (K).

$u[p]$ Standard uncertainty of a measured or predicted property 'p'. The analogous property $U[p]$, which occurs in the Supporting Information, is the expanded uncertainty (equal to $2u[p]$).

γ_X Activity coefficient of species X, on a molality basis.

$\gamma_{\text{HCl}}^{(\text{tr})}$ Trace value of the mean activity coefficient of HCl (in pure artificial seawater, containing no added HCl).

$\gamma_{\text{HCl}}(\text{Stoic.})$ The stoichiometric mean activity coefficient of HCl (also written $\gamma(\text{HCl})_{\text{Stoic.}}$ in Fig. 6). This is based upon the total H^+ and Cl^- molalities in solution (irrespective of equilibria such as the formation of HSO_4^-). Thus the $\text{H}^+ \cdot \text{Cl}^-$ activity product in solution, which is given by $m\text{H}^+ \cdot m\text{Cl}^- \cdot \gamma_{\text{HCl}}^2$ on a free ion basis, can also be expressed as $(m\text{H}^+ + m\text{HSO}_4^-) \cdot m\text{Cl}^- \cdot \gamma_{\text{HCl}}(\text{Stoic.})^2$ in the solutions of interest in this study.

ϕ Molal osmotic coefficient of a solution.

$\Delta\phi$ The difference between measured osmotic coefficients of aqueous NaCl (from various sources) and values calculated using the thermodynamic model of Archer (1992), and shown in Fig. 1 of this work.

$\phi_{\text{sim}}(i)$ Simulated osmotic coefficient measurement i, consisting of three components: a model-calculated true value ($\phi_{\text{mod}}(i)$), plus a systematic error (a term in $\Delta\phi_{\text{sys}}(i)$) and a random error (a term in $\Delta\phi_{\text{rdm}}(i)$), see Eq. (1).

δ_{sys} , ϵ_{rdm} , and η_{rdm} The empirically determined parameters used in the calculation of systematic and random error contributions to a simulated osmotic coefficient measurement $\phi_{\text{sim}}(i)$ above (see Eqs. (2) and (3)).

standard seawater (which also contains additional solutes including fluoride, and various borate and carbonate species), and can also be extended to include the buffers used to define the 'total' pH scale (Hansson, 1973; DelValls and Dickson, 1998). These buffers are solutions of artificial seawater containing equimolar Tris (or THAM, 2-amino-2-hydroxymethyl-1,3-propanediol, CAS 77-86-1) and its conjugate acid TrisH^+ (DelValls and Dickson, 1998). Accurate seawater speciation models, with quantified uncertainties, have applications in several areas: calculations of carbonate equilibria, especially in natural

waters differing from seawater composition; conversions between pH on the total scale (a measure of the sum $[\text{H}^+] + [\text{HSO}_4^-]$) and H^+ concentration and activity; and in calculations of trace metal speciation in natural waters (e.g., Pierrot and Millero, 2016). For pH, the models can assist in the extension of the total scale to lower salinities, and the development of pH standards for saline waters containing the ions of seawater but in different ratios to those in standard seawater. The use of Pitzer-based speciation models has also been suggested in order to address metrological issues concerning the total pH scale (Dickson et al.,

2016).

However, the speciation models referred to above do not yet agree to within experimental uncertainty with available thermodynamic measurements that can be used for validation (chiefly electromotive forces (EMFs) of acidified artificial seawater), nor do they include uncertainty estimates. Indeed, no comprehensive Pitzer model does so.

Quantification of the uncertainty of the model outputs (speciation and solute and solvent activities, and quantities calculated from them) is essential if the speciation models are to be used in the applications noted above. The estimation of uncertainties ideally requires that the variances and covariances of all Pitzer interaction parameters are known, based upon the statistics of the fits to the original thermodynamic measurements and taking account of their experimental uncertainties. The uncertainties associated with each thermodynamic equilibrium constant should also be known. These quantities, together with standard error propagation techniques, allow both the total uncertainty in speciation model outputs to be calculated and also the individual contributions of all parameters and equilibrium constants. The latter are needed to identify the chemical systems for which new measurements are required, or existing data (and the applicable Pitzer interaction parameters) need to be reassessed. Spitzer et al. (2011) and Meinrath (2002), working on models of very simple solutions, have pointed out some difficulties notably the fact that uncertainties of Pitzer parameters are rarely stated in the studies that determine their values from thermodynamic data.

We have addressed the above problems by implementing the Waters and Millero (2013) and Clegg and Whitfield (1995) Pitzer-based speciation models of artificial seawater within a generalised framework for solutions of arbitrary complexity and including full propagation of uncertainties. The Pitzer interaction parameters and equilibrium constants are documented, ambiguities resolved where possible, and some corrections made. The models are compared with the available EMF data for acidified artificial seawater, including the standard EMFs that are essential to the definition of the pH scale used by oceanographers (Dickson, 1990; DelValls and Dickson, 1998). Because there are no available uncertainties for the Pitzer interaction parameters (which are drawn from many different sources) we have adopted a simplified approach to quantify consistently their variances and covariances. This provides indicative uncertainties in model-calculated outputs, enables us to estimate individual uncertainty contributions, and to identify those seawater components for which a rigorous treatment of Pitzer parameter uncertainties is needed. Finally, we discuss the chemical systems (pure solutions and mixtures) for which new measurements need to be made, or existing data reassessed, to improve the models and meet the needs of oceanographers.

2. Speciation models of artificial seawater

Chemical speciation models, based upon the Pitzer equations for activity coefficients, have been developed by Campbell et al. (1993) in a study describing Harned cell measurements of acidified artificial seawater, and by Clegg and Whitfield (1995) in a modelling study of NH_4^+ dissociation in natural waters. Later, Millero and Pierrot (1998) presented a model of standard seawater that includes borate and carbonate equilibria, and Waters and Millero (2013) developed a model of artificial seawater focused on the calculation of pH, and in particular the use of a 'free' pH scale (equivalent, on a molality basis, to $-\log_{10}(m\text{H}^+)$). This model is applicable from 0 to 45 °C, from salinities 5 to 40, and for 1 atm pressure. The model of Clegg and Whitfield (1995) is for solutions of artificial seawater including trace species NH_4^+ and NH_3 , and is intended for use from 0 to 40 salinity, and from -2 to 40 °C (and for 1 atm pressure).

The Pitzer expressions for excess Gibbs energy and osmotic and activity coefficients of arbitrarily complex electrolyte mixtures are given by Pitzer (1991), and by Clegg et al. (1994) who include a generalised form of an additional term used by Archer (1992) in his treatment of the

thermodynamic properties of aqueous NaCl. The equations are not reproduced here. Briefly, activity coefficients are calculated as a summation of the effects of interactions between pairs and triplets of solute species. Each interaction is characterised by one or more parameters, whose values vary with both temperature and pressure. They are determined by fitting to thermodynamic data for aqueous solutions that yield solvent or solute activities, thermal properties (for variations with respect to temperature), or volumetric properties (for variations with respect to pressure) (Pitzer, 1991). The parameters for solutions containing only ions are: $\beta_{ca}^{(0)}$, $\beta_{ca}^{(1)}$, $\beta_{ca}^{(2)}$, $C_{ca}^{(0)}$, and $C_{ca}^{(1)}$ for combinations of each cation c and each anion a ; $\theta_{cc'}$ and $\psi_{cc'a}$ for each pair of dissimilar cations c and c' , and anion a ; and $\theta_{aa'}$ and $\psi_{aa'c}$ for each pair of dissimilar anions a and a' , and cation c . Not all of the five possible cation-anion interaction parameters are generally required. The parameter types are summarised in the glossary of symbols.

The above models are based upon many of the same thermodynamic measurements, made over decades, and draw extensively on previous Pitzer model studies, notably those of Weare and co-workers (e.g., Harvie et al., 1984; Møller, 1988; Greenberg and Møller, 1989). We have adopted the work of Waters and Millero (2013) (noting the corrigendum of Waters et al., 2014) and Clegg and Whitfield (1995) as the base models for this study. They differ chiefly in the numbers of ion interactions to which parameters are assigned, and in the values (including the variation with temperature) of those parameters. The two models are summarised in the Supporting Information, which includes tables of parameter values and temperature coefficients, and calculated properties of various solutions for validation purposes. We have also documented the original sources of the interaction parameters and equilibrium constants and have resolved ambiguities where possible. A few corrections have been made to the model of Waters and Millero (2013), notably for interactions between H^+ and Na^+ , and H^+ and Mg^{2+} . In particular, the parameter $\theta_{\text{H,Na}}$ was re-derived as a function of temperature, from data for $\text{H}^+\text{-Na}^+\text{-Cl}^-$ aqueous solutions (see the Supporting Information). All further references to the model in this work are to the corrected version. When programming the model of Clegg and Whitfield (1995) it was found that a temperature coefficient of the interaction parameter $\beta_{\text{Mg,SO4}}^{(2)}$ was in error, and this also has been corrected.

Pitzer-based models of multicomponent electrolyte solutions are complex, and involve many interactions and parameters. The models of artificial seawater considered here involve potentially twenty four cation-anion interactions (parameters $\beta_{ca}^{(0-2)}$ and $C_{ca}^{(0,1)}$) twenty one like sign interactions (parameter $\theta_{cc'}$ or $\theta_{aa'}$), and ninety six interactions between two ions of one sign and one ion of the opposite sign (parameter $\psi_{cc'a}$ or $\psi_{aa'c}$). Because of this complexity it is not always possible to determine why the model disagrees with particular sets of measurements, or which interactions have the greatest influence on a calculated speciation or activity. Nor is there any direct estimation of overall uncertainty. Clegg and Whitfield (1995) carried out simple sensitivity calculations by determining the changes in the predicted activity coefficients of H^+ , NH_4^+ , and NH_3 in artificial seawater media caused by fractional changes in the molalities of the major ions in order to determine the principal controls of ammonia speciation. However, such approaches are indirect, do not include a consideration of uncertainties, and results are difficult to interpret in complex solutions involving multiple equilibria.

In order to improve current speciation models, and make them more useful for important applications such as pH, it is necessary to be able to estimate both the total uncertainty of any calculated quantity (such as pH, activity, or stoichiometric dissociation constant), and the individual contributions of thermodynamic equilibrium constants and Pitzer model interaction parameters. The fact that these interaction parameters are not independent of one another must also be taken into account. In the next section we describe the inclusion of these capabilities, for the first time, in a Pitzer-based speciation model.

3. Methods

The two models of artificial seawater involve three chemical equilibria: the dissociation of HSO_4^- ($\text{HSO}_4^- \rightleftharpoons \text{H}^+ + \text{SO}_4^{2-}$), that of water ($\text{H}_2\text{O} \rightleftharpoons \text{H}^+ + \text{OH}^-$), and the formation of the MgOH^+ ion pair ($\text{Mg}^{2+} + \text{OH}^- \rightleftharpoons \text{MgOH}^+$). They are solved iteratively to obtain the equilibrium speciation and ion and solvent activities, using techniques that are described in the Supporting Information.

Uncertainties of model-calculated properties can be determined by standard methods of error propagation such as used by Orr et al. (2018) with models of the marine carbonate system if values of the variances and covariances of the Pitzer interaction coefficients, and uncertainties of equilibrium constants in the model, are known. There are none available for the interaction parameters in either the Waters and Millero (2013) model or that of Clegg and Whitfield (1991) (they are rarely specified in any study), and it would be impractical to attempt to re-derive the models to determine them. It is therefore necessary to adopt a simplified approach to estimating parameter variances and covariances, with the expectation that those which contribute the most to the uncertainty of model-calculated properties can later be evaluated individually. Such a simplified approach should be sufficient to identify those interactions and parameters that need revision (perhaps from new experimental measurements) to improve the accuracy of the models, and to provide estimated or indicative uncertainties in model outputs.

Interaction parameters for pure aqueous electrolyte solutions ($\beta_{\text{ca}}^{(0,2)}$, $C_{\text{ca}}^{(0,1)}$) at an individual temperature are typically determined from, (i) solvent activities from isopiestic, vapour pressure, freezing point or boiling point experiments (although the final two require thermal data to adjust the activities to a single temperature); (ii) solute activities from EMF measurements of various electrochemical cells, of which the most important for the present work is the Harned cell (see section 4) which yields the activity product $a\text{H}^+ \cdot a\text{Cl}^-$. The values of ‘mixture’ parameters (θ_{cc} , $\psi_{\text{cc'a}}$, $\theta_{\text{aa'}}$, and $\psi_{\text{aa'c}}$) can be determined from the same types of measurement, and also from solubilities of salts in solution mixtures (e.g., Harvie et al., 1984). In this work we assume that, for all single solute solutions and mixtures for which there are interaction parameters, their values have been determined from single datasets of osmotic coefficients (ϕ) subject to the random and systematic errors that are typical of isopiestic measurements. Osmotic coefficients were adopted because a simple approach was needed for the comprehensive uncertainty analysis undertaken here, and because isopiestic measurements are a principal method of activity measurement for solutions of non-volatile electrolytes and other solutes at room temperature and above (Rard and Platford, 1991). These include all of those salts present in artificial seawater. Thus, variances and covariances based on the assumption of osmotic coefficient datasets can be expected to be representative of many of the cation-anion interactions that most affect the solute activity coefficients and speciation in seawater. It is our assessment that osmotic coefficients constitute more than 75% of the total datasets for single solute solutions at 25 °C, but less than 50% for mixtures (although they have been measured for mixtures of some of the solutes that have the highest concentrations in seawater, or those that are important for the calculation of acid-base equilibria).

We have estimated variances and covariances of the Pitzer interaction parameters in the Waters and Millero (2013) model at the single temperature of 25 °C. We expect the values for the Clegg and Whitfield (1995) model to be similar. Compared to other temperatures, errors and uncertainties at 25 °C are likely to be smaller because of the greater number of measurements and datasets available. The following procedure was adopted: first, variances and covariances of parameters for pure aqueous electrolyte solutions ($\beta_{\text{ca}}^{(0,2)}$, $C_{\text{ca}}^{(0,1)}$) were estimated using a Monte Carlo method in which model-generated osmotic coefficients were perturbed randomly according to defined errors and refitted (repeated many times). Second, taking the pure electrolyte parameters as fixed, the same procedure was carried out for mixtures of

Table 1

Values of the second dissociation constant of H_2SO_4 ($K(\text{HSO}_4^-)$ / mol kg⁻¹) at 25 °C.

$K(\text{HSO}_4^-)$	Uncertainty	Type	Reference
0.0103	–	expt. ^a	Lietzke et al. (1961)
0.01028	0.0002	expt.	Marshall and Jones (1966)
0.01017	0.0002 to 0.0006	expt.	Young et al. (1978)
0.0103	–	expt.	Matsushima and Okuwaki (1988)
0.01039	0.00018	expt.	Mussini et al. (1989)
0.01043	0.0002	expt.	Mussini et al. (1989)
0.01086	0.0005	expt.	Dickson et al. (1990)
0.0105	–	model ^b	Pitzer et al. (1977)
0.01036	–	model ^c	Hovey and Hepler (1990)
0.0105	–	model ^d	Clegg et al. (1994)
0.01058	–	model ^e	Knopf et al. (2003)
0.0119	0.0012	model ^f	Sippola and Taskinen (2014)
0.0105	0.0005	model ^g	this work

Notes: The ‘Type’ column indicates whether the value of $K(\text{HSO}_4^-)$ is determined primarily from experimental measurements that, directly or indirectly, yield values of the equilibrium constant (‘expt.’) or are determined by the application of the Pitzer activity coefficient model to activity and thermal data (‘model’).

^a Determined from the application of a model to literature data for solubilities.

^b Largely determined by the application of the Pitzer model (without unsymmetrical mixing terms) to literature data for emfs. The quoted value of 0.0105 is favoured, but an alternative model treatment yielding a value of 0.0120 was also found to be possible.

^c These authors adopted the equation of Pitzer et al. (1977) for $K(\text{HSO}_4^-)$, and added a $\Delta_r C_p^\circ$ (heat capacity) term.

^d Clegg et al. (1994) adopted Eq. (6) of Dickson et al. for $K(\text{HSO}_4^-)$ (terms in p_1 to p_5), but added a fixed increment in $\log_{10}(K(\text{HSO}_4^-))$ at all T to yield exactly 0.0105 mol kg⁻¹ at 25 °C.

^e Knopf et al. (2003) fitted a range of activity and thermal data, and their own experimentally determined degrees of HSO_4^- dissociation. Osmotic coefficients and vapour pressures were omitted, and some of the emfs (yielding H_2SO_4 activities) are known to be inaccurate (Rard and Clegg, 1995).

^f Sippola and Taskinen (2014) fitted a range of activity and thermal data (but omitting heat capacities), and their expression for $K(\text{HSO}_4^-)$ as a function of temperature lacks a $\Delta_r C_p^\circ$ (heat capacity) term.

^g The model of Clegg et al. (1994) is used, with the uncertainty taken from the study of Dickson et al. (1990).

two electrolytes containing a common ion to obtain variances and covariances of parameters θ_{cc} and $\psi_{\text{cc'a}}$ (or $\theta_{\text{aa'}}$ and $\psi_{\text{aa'c}}$). The determination of the functions defining the errors, and their application to obtain parameter variances and covariances, are described in the next section. Further details of the sequence in which uncertainties of the model parameters were estimated are given in the Supporting Information.

The interaction parameters that are set to zero in the models (often because there are no data from which they can be evaluated) fall into several different categories, which are discussed in the Appendix. Those that are likely to be non-zero can be assigned values, and associated standard deviations, determined by averaging results from literature studies covering many solutes and mixtures. The variance of the principal equilibrium constant in the model, for the dissociation of HSO_4^- , was taken from the literature, see Table 1. The value for the association constant for the ion-pair MgOH^+ is equal to 154.2 ($\text{p}K = -2.19$, or $\ln(K) = 5.043$) at 25 °C (Harvie et al., 1984), and its standard uncertainty was estimated to be ± 0.022 in $\ln(K)$. Variances of both the equilibrium constants, that of the dissociation of water, and some further details are listed in the Supporting Information.

The approach to the estimation of variances and covariances outlined above corresponds to how Pitzer-based chemical speciation models of solution mixtures are typically developed, but it does not capture all types of model uncertainty. First, there are limits to the maximum molalities to which osmotic and activity can be represented accurately (about 6 mol kg⁻¹ for many electrolytes containing singly charged ions). While this is not directly a limitation at seawater ionic

strengths, fits over extended ranges of concentration can result in reduced accuracy at all molalities. Second, mixture parameters $\theta_{ii'}$ and $\psi_{ii'j}$ (where i and i' are dissimilar ions of one sign, and j is an ion of the opposite sign) are often determined from measurements at high molalities, at which their influence is greatest, and errors in the representation of the cation-anion interactions from the pure solution parameters will be reflected in the fitted values of $\theta_{ii'}$ and $\psi_{ii'j}$. The same problem is apparent when the mixture parameters are used with sets of pure solution parameters different from the ones they were originally determined with. It is important to note that systematic errors will be introduced into model calculations at temperatures other than 25 °C if there are strong interactions for which the variation of the Pitzer parameters (or equilibrium constants) with temperature is not known. Such errors are not accounted for in the parameter variances that we have determined here, and we have confined our analysis of uncertainties to 25 °C.

Next we describe the determination of the functions characterising the errors typical of isopiestic experiments, their application within a Monte Carlo approach to determine the variances and covariances of the interaction parameters, and the error propagation method used to calculate the corresponding uncertainty in model-calculated outputs.

3.1. Errors and uncertainties of osmotic coefficients

The isopiestic method, described in detail by Rard and Platford (1991), involves the equilibration of the solvent activities of test and reference solutions (by vapour transfer) in a sealed chamber at constant temperature. After equilibration, the molalities of both sets of solutions are determined by weighing, and the osmotic coefficients of the test solutions calculated from those of the reference (see eq. 32 of Rard and Platford).

Osmotic coefficients are subject to both random measurement errors that affect each data point differently, and systematic errors that affect the entire dataset consistently. The latter might be caused, for example, by incomplete equilibrium in the isopiestic chamber (although we recognise that the degree of disequilibrium might vary between sample cups). For each measurement i , at molality $m(i)$, in an artificial dataset we simulate both a random and a systematic measurement error. These are then added to the osmotic coefficient calculated by the model ($\phi_{\text{mod}}(i)$) to obtain a simulated measurement ($\phi_{\text{sim}}(i)$):

$$\phi_{\text{sim}}(i) = \phi_{\text{mod}}(i) + D \cdot \Delta\phi_{\text{sys}}(i) + H(i) \cdot \Delta\phi_{\text{rdm}}(i) \quad (1)$$

where $\phi_{\text{mod}}(i)$ is the osmotic coefficient calculated by the model for molality $m(i)$. The quantities $\Delta\phi_{\text{sys}}(i)$ and $\Delta\phi_{\text{rdm}}(i)$ are, respectively, measures of the systematic and random errors for the same molality. These quantities are calculated using three empirical parameters (δ_{sys} , ϵ_{rdm} , and η_{rdm}):

$$\Delta\phi_{\text{sys}}(i) = \delta_{\text{sys}}(1 + 1/(m(i) + 0.03)) \quad (2)$$

$$\Delta\phi_{\text{rdm}}(i) = (\epsilon_{\text{rdm}} + \eta_{\text{rdm}}/(m(i) + 0.03)) \quad (3)$$

The forms of these equations (notably the use of the denominator $(m(i) + 0.03)$) reflect the fact that errors in osmotic coefficients from isopiestic experiments increase at low molalities, because of the relationship between water activity and osmotic coefficient. The D and $H(i)$ coefficients in Eq. (1) are simulated by a pseudorandom number generator (Mersenne twister). They have the following distributions:

$$D \sim N(0, 1) \quad (4)$$

$$H(i) \sim N(0, \pi/2) \quad (5)$$

These expressions have the following meanings: the value of D is drawn, once for each artificial dataset, from a normal distribution (N) with a mean of 0 and variance of 1. A value of $H(i)$ is drawn, once for each measurement i , from a normal distribution with a mean of 0 and variance of $\pi/2$. The use of the variance of $\pi/2$, rather than unity, reflects

that fact that parameter ϵ_{rdm} is determined as a mean absolute deviation, which must be multiplied by the factor $(\pi/2)^{0.5}$ to obtain the equivalent standard deviation (and $(\pi/2)^{0.5}N(0,1)$ is equal to $N(0, \pi/2)$).

In this study, we used constant values of $\delta_{\text{sys}} = 0.00116$, $\epsilon_{\text{rdm}} = 0.003$ and $\eta_{\text{rdm}} = 0$ in the simulations. They represent the average random and systematic offsets in our analysis of real osmotic coefficients of multiple electrolyte pairs. We illustrate this analysis here using the electrolytes KCl and NaCl, which have been extensively studied and for which comprehensive evaluations of their thermodynamic properties exist (Archer, 1992; 1999).

Fig. 1a shows the difference between osmotic coefficients of aqueous NaCl determined from measured isopiestic ratios against aqueous KCl (with aqueous KCl osmotic coefficients calculated from Archer, 1999), and those calculated directly from the thermodynamic model of Archer (1992) for aqueous NaCl for the same molalities. Values of $\Delta\phi$ shown on the plot can be fitted with Eq. (2) to obtain δ_{sys} for each of the six individual datasets shown. For use in Eq. (1) δ_{sys} would then be set equal to the standard deviation of these values (0.000292) about a mean of zero, if only considering data for NaCl-KCl aqueous solutions. The dashed lines in Fig. 1a show $\Delta\phi_{\text{sys}}(i)$ calculated using this result and Eq. (2). The solid lines show the result using the larger value of δ_{sys} (0.00116) determined using the complete dataset of many electrolyte pairs. Fig. 1b shows absolute values of $\Delta\phi$ from part (a), but with systematic offsets (calculated using individual fits of Eq. (3) to each dataset) subtracted. The mean value for these datasets is indicated by the dashed line, and the solid line shows the value (ϵ_{rdm} equal to 0.003) adopted on the basis of our study of data for the full range of electrolyte pairs, and the assessment of Rard and Platford (1991).

The systematic component of error δ_{sys} was estimated from 24 isopiestic datasets involving combinations of NaCl, KCl and CaCl₂. Values of δ_{sys} from the majority of the datasets are well represented by a normal distribution, for δ_{sys} within the range $\pm 4 \times 10^{-3}$. The presence of a few outliers (only 3 out of 24 separate studies) indicates that sometimes larger systematic errors occur. However, there is at present insufficient evidence to support using any other distribution, and the Gaussian distribution is the best option due to the central limit theorem. The random deviations, whose absolute values are shown in Fig. 1b, conform to a normal distribution if 8 values out of a total of 205 are omitted. These values of $|\Delta\phi - \delta_{\text{sys}}(1 + 1/(m + 0.03))|$ are all greater than about 3 times the mean shown in the figure (dashed line), and are mostly at low molalities for which very small deviations from equilibrium in the isopiestic apparatus produce large errors in the osmotic coefficient. Data such as these would typically be omitted – as obviously erroneous – from fits of osmotic coefficients to obtain Pitzer model parameters.

3.2. Variances and covariances of the Pitzer interaction parameters

We first consider pure aqueous solutions containing hypothetical electrolytes consisting of every cation-anion pair in the model for which there are non-zero ($\beta_{\text{ca}}^{(0-2)}$, $C_{\text{ca}}^{(0,1)}$) parameters. Artificial datasets of osmotic coefficients were generated, and variances and covariances determined, as follows: (i) for each solute a realistic measurable range of molality m_{min} to m_{max} is first defined. The value of m_{min} is set to a practical lower limit of isopiestic measurements (0.2 mol kg^{-1}), and m_{max} generally to the solubility of the solute (but never greater than 6 mol kg^{-1}). (ii) We assign a set of N_{meas} measurements per dataset, evenly spaced from m_{min} to m_{max} with respect to \sqrt{m} because this yields values that are typical of real experiments. In this work N_{meas} is equal to 50, and we assume a single dataset for simplicity. (The use of multiple datasets significantly reduces simulated uncertainties.) (iii) Next, the osmotic coefficient at each molality is calculated, and sets of systematic and random measurement errors determined using Eqs. (1) to (5) are added to the modelled osmotic coefficients, which are then fitted to obtain a new set interaction parameters. These simulation and fitting steps are repeated many times (typically 10^4) and, finally, variances and

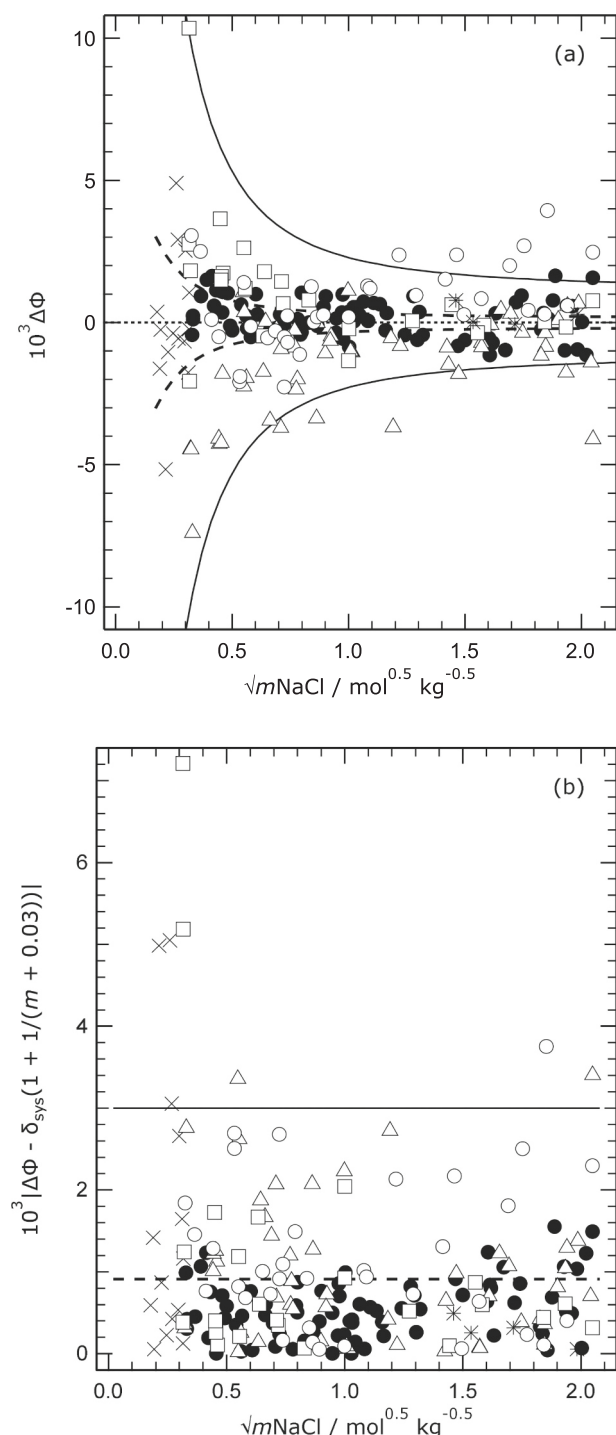


Fig. 1. (a) The difference ($\Delta\phi$) at 25, 30, and 35 °C, between osmotic coefficients of aqueous NaCl determined from measured isopiestic ratios against aqueous KCl, and calculated directly from the thermodynamic model of Archer (1992) for aqueous NaCl for the same molalities. The thermodynamic properties of the aqueous KCl reference were calculated from Archer (1999). Symbols: dot – Robinson (1945); cross – Gordon (1943); circle – Robinson and Sinclair (1934); square – Scatchard et al. (1938); star – Kirgintsev and Lukyanov (1967); triangle – Janis and Ferguson (1939). Lines: solid – systematic offset calculated from Eq. (2) using the mean $|\delta_{\text{sys}}|$ for many datasets (not shown); dashed – the same as the solid line but calculated using the mean $|\delta_{\text{sys}}|$ for the datasets for NaCl/KCl shown in this figure. (b) The absolute value of $\Delta\phi$ less the expression for systematic offset (Eq. (2), fitted to each dataset individually). Symbols: the same sources as in (a). Lines: solid – average random offset (ϵ_{rdm}) calculated from results for many datasets (not shown); dashed – the same as the solid line but calculated only for the datasets for NaCl/KCl shown in this figure.

covariances of the interaction parameters across all steps are evaluated and then saved as a matrix of values. This matrix is later used to propagate the uncertainty associated with the corresponding set of interaction parameters through the Pitzer model to any of its output quantities.

Second, there are ternary interactions for mixtures of two electrolytes with a common ion (parameters $\theta_{\text{cc}'}^{\text{c}}$ and $\psi_{\text{cc}'\text{a}}^{\text{c}}$, or $\theta_{\text{aa}'}^{\text{c}}$ and $\psi_{\text{aa}'\text{c}}^{\text{c}}$). The procedure for determining variances and covariances is similar to that described above. There is now a pair of (m_{min} , m_{max}) values, and the N_{meas} solution compositions (25) are assigned in five groups each of which has a nearly constant molality ratio of the two solutes (resembling typical experiments). Variances and covariances of ($\theta_{\text{cc}'}^{\text{c}}$ and $\psi_{\text{cc}'\text{Cl}}^{\text{c}}$) and ($\theta_{\text{aa}'}^{\text{c}}$ and $\psi_{\text{aa}'\text{Na}}^{\text{c}}$) are determined first, from simulations of electrolyte mixtures containing Cl^- and Na^+ counterions, respectively. The variances of each $\theta_{\text{cc}'}^{\text{c}}$ determined in this way were then used in further simulations to obtain those of all $\psi_{\text{cc}'\text{a}}^{\text{c}}$, where anion a is any anion except Cl^- . The same approach was applied to obtain variances of $\psi_{\text{aa}'\text{c}}^{\text{c}}$ (where c is any cation except Na^+). It is a consequence of this approach, which is analogous to how parameter values themselves are determined, that there are no covariances between different $\psi_{\text{cc}'\text{a}}^{\text{c}}$, or $\psi_{\text{aa}'\text{c}}^{\text{c}}$.

The assumption of a single simulated dataset for pure aqueous solutions represents a worst case (there are more sets of measurements in most cases). The smaller number of simulated measurements (N_{meas}) for mixtures, compared to single solute solutions, is typical. The further assumption that all data are from isopiestic experiments will tend to yield overestimates of uncertainties, particularly at low molalities where the isopiestic technique is less accurate. In practice, data from a variety of thermodynamic measurements are included in determinations of Pitzer model parameters and they have different relationships between solution molality and measurement uncertainty. For example, EMF measurements are especially important sources of data of aqueous HCl and its mixtures with metal chlorides, and freezing point depressions can yield accurate values of water activity for very dilute solutions of many solutes. Using such data together with osmotic coefficients from isopiestic measurements would reduce the uncertainties of fitted parameters and those of model outputs. However, it is important to note that although the value of m_{min} is higher than the molalities of many of the components present in seawater – especially if diluted – the uncertainties in the values of the Pitzer parameters (and consequently model outputs) are constrained by the fact the osmotic and all activity coefficients closely approach the Debye-Hückel limiting law, for which the Pitzer model contains appropriate expressions, as ionic strength decreases. The effect of this can be seen in plots in the Supporting Information associated with section 3.4, below.

Details of the simulations, the methods used, and the arrangements of values in the uncertainty matrices, are described in the Supporting Information.

3.3. Determination of uncertainties in model outputs

The propagation of uncertainties, to calculate those in model outputs such as EMF, species concentration, or activity, is carried out using a matrix approach as described by Orr et al. (2018). See their Eq. (2) and Eqs. A.1 to A.5. The additional quantities that are required, in addition to the variances and covariances of the parameters and logarithms of the equilibrium constants, are the partial derivatives of the model output quantity with respect to each individual interaction parameter and $\ln(K)$. These are determined numerically, with a centred finite difference formula using two to six points depending upon the accuracy required. The calculation of both the total variance, and the individual parameter and equilibrium constant contributions to it, are summarised in Appendix B of this work.

3.4. Examples: aqueous NaCl and HCl

In the Supporting Information we describe the results of applying the above methods to aqueous NaCl and HCl and compare the calculated

uncertainties to several evaluations (including the models presented in this work) of osmotic and activity coefficients at 25 °C. These two solutes were chosen, first, because NaCl is the major dissolved constituent of seawater, and interactions of dissolved Cl^- with H^+ (calculated using parameters obtained from thermodynamic properties of aqueous HCl) are central to the calculation of pH. Second, both solutions have been extensively studied and their thermodynamic properties are the subject of a number of critical evaluations. For aqueous NaCl, osmotic and mean activity coefficients from the model of Waters and Millero (2013) and from the following studies were compared with values from the critical evaluation of Archer (1992) (which is used in the model of Clegg and Whitfield (1995)): Robinson and Stokes (1970), Clarke and Glew (1985), Gibbard et al. (1974), and Hamer and Wu (1972). For aqueous HCl, calculated Harned cell EMFs and mean activity coefficients from the models of Waters and Millero (2013), Clegg and Whitfield (1995) and the following evaluations were compared with values from Hamer and Wu (1972): Robinson and Stokes (1970), Partanen et al. (2007), and Holmes et al. (1987). The main findings of the above comparisons are as follows:

- (i) Osmotic and activity coefficients of NaCl lie well within the calculated ranges of uncertainty for ionic strengths up to those equivalent to salinity 45 seawater. This suggests that the uncertainty contributions of NaCl, and similarly well-studied electrolytes, to calculated activities in seawater solutions are likely to be conservatively estimated (i.e., somewhat overestimated) by the model.
- (ii) The maximum difference between values of γ_{NaCl} from the Waters and Millero (2013) model, and the equation of Archer (1992), is about 0.001 at seawater ionic strengths. A change of this magnitude in the activity coefficient of the Cl^- ion would correspond to a change of only about 0.04 mV in the EMF of a Harned cell, thus both models agree very closely with each other for Na^+ - Cl^- interactions at seawater ionic strengths.
- (iii) For ionic strengths up to that of seawater, the model of Waters and Millero (2013) probably represents the interactions of H^+ with Cl^- in pure aqueous solution to better than 0.1 mV (equivalent to about 0.002 in γ_{HCl}). The model of Clegg and Whitfield (1995) predicts EMFs that are about 0.05 mV lower (hence γ_{HCl} greater by about 0.001).
- (iv) The estimated uncertainty envelope for predicted EMFs and mean activity coefficients of aqueous HCl appears to be too large at most molalities. There are two main reasons for this: first, mean activity coefficients γ_{HCl} are related to the integral of $(\phi - 1)$ with respect to $m^{1/2}$, which means that model-calculated uncertainties (based upon Pitzer parameters determined only from simulated osmotic coefficient data) increase monotonically with molality, as can be seen in Fig. S4. Second, EMF measurements are a direct measure of HCl activity, with an uncertainty that varies little with molality. Thus an expanded uncertainty in a measured $(E - E^0)$ of 0.08 mV would yield an uncertainty in γ_{HCl} of 0.0012 (0.1 mHCl) and 0.0013 (1.0 mHCl). The calculated uncertainty shown in Fig. S4 is greater than these values by about a factor of 6 for an ionic strength equivalent to seawater of salinity 35 (0.7225 mol kg^{-1}), and the greatest difference in γ_{HCl} between the models and critical evaluations and those of the reference is about a factor of 1.5. This is likely to lead to overestimates of the contribution of H^+ - Cl^- interactions to the uncertainties of calculated HCl activities and Harned cell EMFs used for comparisons in this work, and must be borne in mind when analysing the results. The method of uncertainty estimation described above should in the future be extended to include EMFs of electrochemical cells as a further data type.

Table 2

Sources of electromotive force data.

Salinities	Ionic strengths ^a (mol kg^{-1})	<i>t</i> (°C)	Solution ^b	Ref.
–	0.280–0.879	5–40	HCl + ASW (without SO_4^{2-})	Khoo et al. (1977)
20.31, 34.99, 44.55	0.413–0.929	5–40	HCl + ASW	Khoo et al. (1977)
5–45	0.100–0.939	0–55	HCl + ASW	Campbell et al. (1993)
5–45	0.100–0.939	0–45	HCl + ASW	Dickson (1990)

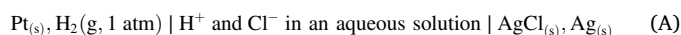
Notes

^a These are formal ionic strengths that do not take into account any ion-pairing (see Khoo et al., 1977) or the formation of HSO_4^- in the solutions of artificial seawater with added HCl.

^b Artificial seawater is denoted by ASW.

4. Data used to assess the models

Calculations of equilibrium chemical speciation require values of the ion activity coefficients in the seawater or other natural water medium. Electromotive force data for acidified artificial seawater are used to evaluate the accuracy of the models, and the uncertainty propagation methods described above are used for two purposes. First, they are applied to compare the uncertainties in model predictions to those of the experimental data. Second, they are used to determine the solute interactions and equilibrium constants most likely to cause the differences between measured and modelled EMFs, and the solute activities derived from them. The sources of data, summarised in Table 2, are for the following electrochemical (Harned) cell:



where the aqueous solution contains acidified artificial seawater. Note that the study of Khoo et al. (1977) includes results for artificial seawater not including the SO_4^{2-} ion. The EMF, E (V), of cell A is given by the following expression:

$$E = E^0 - (RT/F) \cdot \ln(a\text{H}^+ \cdot a\text{Cl}^-) \quad (6)$$

where E^0 (V) is the standard EMF of the cell at the temperature T (K) of interest, R (8.31446 J $\text{mol}^{-1} \text{K}^{-1}$) is the gas constant, F (96,485.332 C mol^{-1}) is Faraday's constant, and prefix a denotes activity. The activity product of the H^+ and Cl^- ions can also be written $m\text{H}^+ \cdot m\text{Cl}^- \cdot \gamma_{\text{H}} \cdot \gamma_{\text{Cl}}$ or $m\text{H}^+ \cdot m\text{Cl}^- \cdot \gamma_{\text{HCl}}^2$, where γ_i is the activity coefficient of solute species i , and γ_{HCl} is the mean activity coefficient of H^+ and Cl^- in the aqueous solution (γ_{HCl} is equal to $(\gamma_{\text{H}} \cdot \gamma_{\text{Cl}})^{0.5}$).

Comparisons of measured and calculated EMFs of acidified artificial seawater without SO_4^{2-} are mainly a test of the ability of the models to represent the interactions of Cl^- with H^+ , and the interactions of the

Table 3

Solution compositions for artificial seawaters (ASW) of salinity 35.

Solute species	ASW, without SO_4^{2-} (mol kg^{-1})	ASW (mol kg^{-1})	ASW (mol kg^{-1})
H^+	– ^a	– ^a	– ^a
Na^+	0.51442	0.48516	0.48618
Mg^{2+}	0.05518	0.05518	0.05474
Ca^{2+}	0.01077	0.01077	0.01075
K^+	0.01058	0.01058	0.01058
Cl^-	0.65690	0.56912	0.56920
SO_4^{2-}	–	0.02926	0.02927

Notes: The compositions in the first two columns of molalities are from Khoo et al. (1977), and the third is from Dickson (1990). Campbell et al. (1993) used the recipe of Dickson (1990).

^a In EMF measurements of acidified artificial seawater, H^+ (of various different molalities) is substituted for Na^+ .

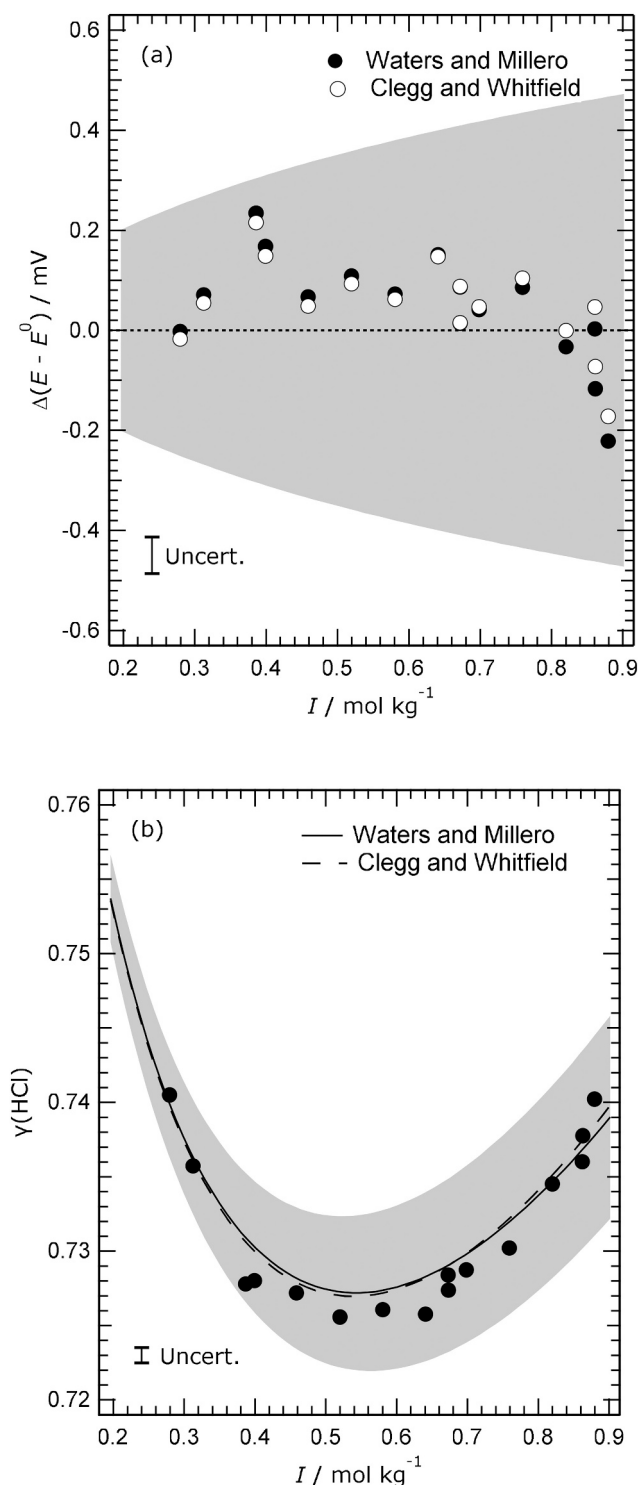


Fig. 2. Measured and modelled properties of acidified artificial seawater without sulphate, at 25 °C. (a) Differences between measured and calculated EMFs ($\Delta(E - E^0)$), Eq. (6), plotted against the ionic strength (I) of the solution. Symbols: dot – measurements of Khoo et al. (1977) minus values calculated using the Waters and Millero (2013) model; circle – the same measurements minus values calculated using the model of Clegg and Whitfield (1995). The shaded area shows the uncertainty in the calculated value of $(E - E^0)$, and is centered on the zero line. (b) Experimental and calculated mean activity coefficients of HCl ($\gamma(\text{HCl})$) plotted against ionic strength. These are the same results as shown in (a). Lines: solid – Waters and Millero model; dashed – Clegg and Whitfield model. The shaded area indicates the uncertainty in the calculated mean activity coefficient. The estimated uncertainties in the measured values of the y variable (i.e., \pm one standard deviation) are also indicated on the plots.

cations of seawater with Cl^- . There are no chemical equilibria considered in these solutions (the influence of the water dissociation reaction is only significant in solutions close to neutral pH, and the $\text{Mg}^{2+} + \text{OH}^- \rightleftharpoons \text{MgOH}^+$ reaction only in neutral and basic solutions). In solutions of acidified artificial seawater including SO_4^{2-} the reaction with H^+ to form HSO_4^- has a large influence on H^+ activity, mainly by reducing the molality of free H^+ in solution. The equilibrium can be expressed as:



The value of the dissociation constant, $K(\text{HSO}_4^-)$, is known only to within about 5% at 25 °C (Dickson et al., 1990), and probably less well at other temperatures. However, the accurate representation of this equilibrium in seawater media is central to the interconversion of pH on the free ($[\text{H}^+]$) and total ($[\text{H}^+] + [\text{HSO}_4^-]$) scales, and to an assessment of the empirically determined standard electromotive force E^* (Dickson, 1990) used in the definition of the “total hydrogen ion” pH scale (DelValls and Dickson, 1998). This is discussed further in section 7. Values and uncertainties of $K(\text{HSO}_4^-)$ from various sources are listed in Table 1.

The published EMF data used in this work for artificial seawater and other solutions are normalized in the original studies to a hydrogen partial pressure of 101.325 kPa according to:

$$E = E_{\text{meas}} - (RT/(2F)) \cdot \ln[(p_{\text{atm}}/\text{kPa} - p_{\text{H}_2\text{O}}/\text{kPa})/101.325] \quad (8)$$

where E (V) is the normalized EMF, E_{meas} is the experimentally determined EMF, p_{atm} is the ambient pressure, and $p_{\text{H}_2\text{O}}$ is the equilibrium partial pressure of water of the test solution. The contributions to the total uncertainty in E arise from those in p_{atm} , $p_{\text{H}_2\text{O}}$, T , and E_{meas} . The uncertainty in the standard EMF E^0 is also important because it is $(E - E^0)$ from which the activity product of H^+ and Cl^- ions is determined (see Eq. (6) above).

To establish a comprehensive estimate of uncertainty for E , E_{meas} was first estimated from the published values of E by solving Eq. (8). Calculations were carried with p_{atm} ranging from 98 kPa to 103 kPa because values of p_{atm} necessary to determine the actual E_{meas} are not stated in the original studies. The contributions of p_{atm} , $p_{\text{H}_2\text{O}}$, R , T and F to the combined standard uncertainty of E were then compared at the different values of p_{atm} , and were found to differ by less than 1 μV . The other elements of the uncertainty analysis were carried out with E_{meas} estimated from E at p_{atm} equal to 101.325 kPa.

The uncertainty in the measured EMF is modeled as two components: the uncertainty $u[E_{\text{DVM}}]$ in the measured result from the digital voltmeter, and the uncertainty arising from the drift in the EMF between initial and subsequent measurements at 298.15 K, $u[E_{\text{T cycling}}]$. A detailed description of the assessment of these elements, and the contributions of $p_{\text{H}_2\text{O}}$, p_{atm} , and T , is given in the Supporting Information together with an example of results for a typical measurement (including uncertainties arising from solution preparation). We find that 99% of the estimated combined standard uncertainty for E is accounted for by $u[E_{\text{DVM}}]$ and $u[E_{\text{T cycling}}]$. The remaining 1% of the total combined uncertainty is almost entirely attributable to $p_{\text{H}_2\text{O}}$.

The uncertainties in the differences between measured EMFs and standard electrode EMF, $(E - E^0)$, are determined using the estimated uncertainty for E summarized above and a fixed standard uncertainty in E^0 of 30 μV (for further details, see the Supporting Information). Based on these results the estimated standard uncertainties in $(E - E^0)$ at 298.15 K are about 0.037 mV for all the measurements (i.e., Khoo et al., 1977; Dickson, 1990; and Campbell et al., 1990). This value is consistent with the observation of Dickson (1990) that measurements made at 298.15 K during individual runs tended to agree within 0.05 mV.

In this work we have found that the agreement between measurements of acidified artificial seawater from the different studies is best at 298.15 K, but tends to decrease towards the temperature extremes (and the scatter increases). Also, other factors related to the preparation and treatment of electrodes, and the operation of the cells, can have effects

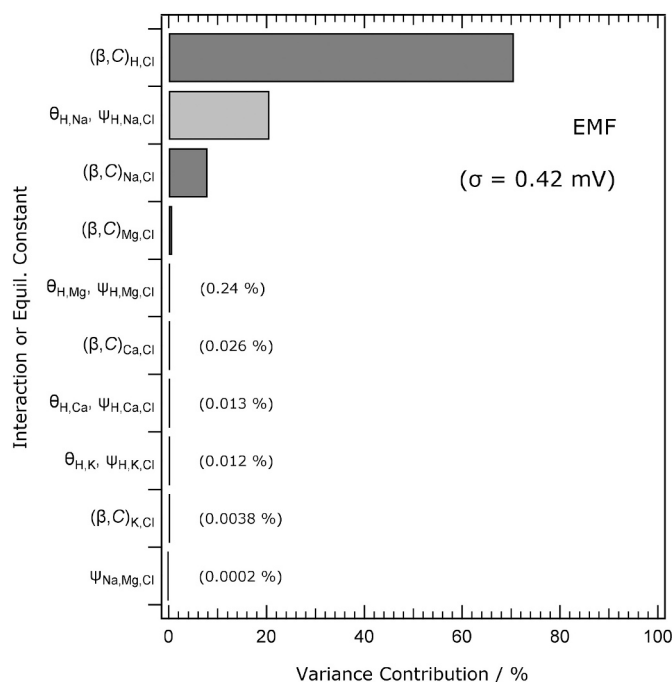


Fig. 3. Percentage contributions of individual Pitzer model interactions to the variance of the calculated EMF (Eq. (6)) at 25 °C of a Harned cell containing artificial seawater without SO_4^{2-} , acidified with 0.01 mH^+ . The parameters associated with each of the interactions are listed down the left hand side, and contributions of <1% are noted on the plot. Interactions with very small variance contributions (below 0.0002%) are omitted. The predicted standard deviation (σ) is 0.42 mV.

on both uncertainty and accuracy that are not accounted for in this analysis. For example, although the results of Khoo et al. (1977) and Dickson (1990) generally agree well and exhibit behavior that is consistent with the standard uncertainties noted above, the measurements of Campbell et al. (1993) are more scattered and data for two solutions were excluded from our analysis because of consistent deviations (of the order of 0.2 mV and above) at all T .

5. Assessment of the Models at 25 °C

In this section we compare the models with available EMF data, and use uncertainty information generated using the methods described earlier to identify causes of the differences found.

5.1. Calculations of uncertainty contributions to modelled quantities

We first carried out model simulations to determine the relative contributions of the equilibrium constants and interaction parameters in the model to uncertainties of calculated EMFs, and H^+ and Cl^- activities and activity coefficients. These simulations were for acidified artificial seawater, both with and without SO_4^{2-} , at 25 °C. The salinity is 35 in both cases, and the compositions of the solutions are listed in Table 3. In the calculations for acidified artificial seawater we use the recipe of Dickson (1990), rather than that of Khoo et al. (1977), because it is the former that has been used in experiments to define pH on the total scale (DelValls and Dickson, 1998). The model of Waters and Millero (2013) was used in all uncertainty simulations.

Two sets of simulations were carried generally out. In the first set the variances and covariances of parameters whose values are set to zero in the model are also set to zero. These parameters are listed in Tables S2 to S4 in the Supplementary Information and include, for example, $\theta_{H_2SO_4, SO_4}$ and those for interactions between pairs of reacting species such as H^+ and $MgOH^+$. There are also parameters for

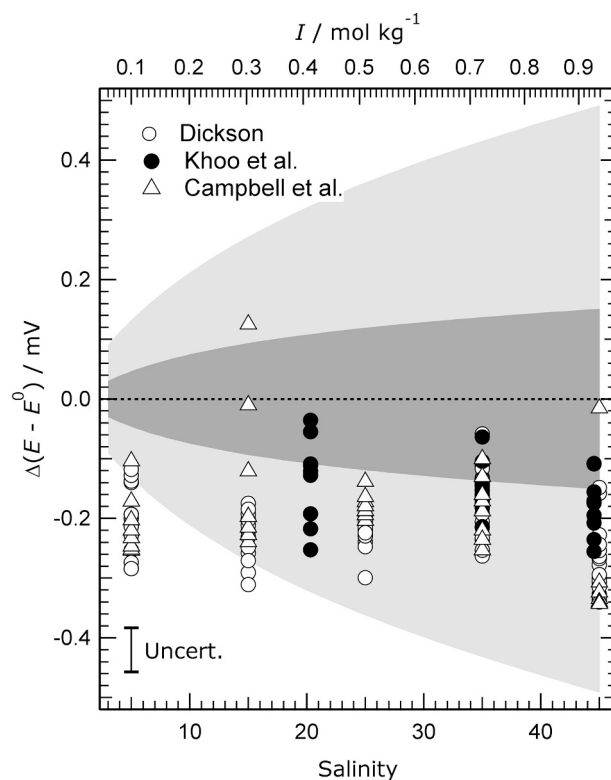


Fig. 4. Measured and modelled properties of acidified artificial seawater, at 25 °C. (a) Differences between measured and calculated EMFs ($\Delta(E - E^0)$), calculated using the model of Waters and Millero (2013), plotted against salinity (bottom axis) and ionic strength (I) (top axis). Symbols: circle – measurements of Dickson (1990); dot – measurements of Khoo et al. (1977); triangle – measurements of Campbell et al. (1993). The lighter shaded area shows the total uncertainty in the calculated values of $(E - E^0)$, and is centered on the zero line. The inner, darker, shaded area is the uncertainty attributed to that of the thermodynamic dissociation constant of HSO_4^- . The estimated uncertainty in the measured values of $(E - E^0)$ (i.e., \pm one standard deviation) is indicated on the plot.

interactions that are unknown because of a lack of data from which to determine them. These are assigned values of zero by default, but may be non-zero. Their variances and covariances are simulated in the same way as described for the other parameters.

The second set of uncertainty simulations is intended to explore the influence of model parameters whose values are unknown, but may not be zero (identified by 'U' in Tables S2 to S4). In this case we have substituted mean parameter values (for charge types corresponding to those of the interacting ions) from Tables A1 and A2 in the Appendix, and set their variances equal to the squares of the standard deviations. We have not attempted to estimate covariances of, for example, θ_{ij} and ψ_{ij} parameters whose values are generally determined simultaneously. This will tend to increase their contributions to the total calculated uncertainty. This substitution of non-zero parameter values into the model means that the calculated quantities – both speciation and activity coefficients – will be different from the base model. However, the differences have been found to be very small.

5.2. Acidified artificial seawater without sulphate

Khoo et al. (1977) replaced SO_4^{2-} with charge-equivalent amounts of Cl^- when preparing these solutions. The composition is given in Table 3. Fig. 2 shows the difference between measured and modelled EMFs, and the same data as mean activity coefficients of HCl. The principal uncertainty contributions to the calculated $(E - E^0)$, at ionic strength 0.7228 $mol\ kg^{-1}$, are displayed in Fig. 3. The partial derivatives

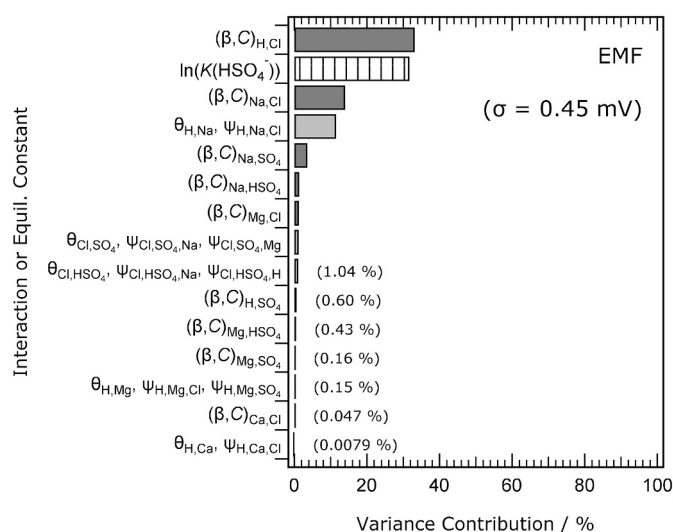


Fig. 5. Percentage contributions of individual Pitzer model interactions, and equilibrium constants, to the variance of the calculated EMF (Eq. (6)) at 25 °C of a Harned cell containing artificial seawater, acidified with 0.01 mH^+ . The parameters associated with each of the interactions are listed down the left hand side, and contributions of about 1% and below are noted on the plot. Interactions with very small variance contributions (below 0.0079%) are omitted. The predicted standard deviation (σ) is 0.45 mV.

of the calculated ($E - E^0$) with respect to each parameter are shown in Fig. S1 of the Supporting Information. Both these results show that H^+-Cl^- and Na^+-Cl^- interactions, and the parameters $\theta_{H,Na}$ and $\psi_{H,Na,Cl}$, dominate the uncertainty in the modelled EMF, which is to be expected given that NaCl constitutes 86% (on a molar basis) of the dissolved solutes. As is also the case for H^+-Cl^- interactions, the parameters $\theta_{H,Na}$ and $\psi_{H,Na,Cl}$ are determined from EMF data, and so their uncertainty contribution may be overestimated for reasons given in section 3.4. However, this does not change the conclusion that the three sets of interactions account for most of the total calculated uncertainty. Separate calculations of EMFs and uncertainty contributions using the averaged parameter values (see the Appendix) in place of those that are unknown yielded identical results to those shown. This is because, for this system, they involve only the ions $MgOH^+$ and OH^- which have no influence on speciation or activities in these acidic solutions.

The measured EMFs and γ_{HCl} in Fig. 2 lie within the uncertainty envelope of the modelled values. As described above, this is likely to be too large given that H^+-Cl^- and $H^+-Na^+-Cl^-$ interactions are calculated to contribute the most (90% of the total variance, Fig. 3) and we have already shown that the assumption of an osmotic coefficient data set for the determination of Pitzer H^+-Cl^- parameters appears to overestimate the uncertainties of HCl activity coefficients in pure aqueous HCl as shown in the Supporting Information. An overestimate of the calculated uncertainty in Fig. 2 of a factor of 2 to 3 is consistent with what was found for aqueous HCl.

The comparisons in Fig. 2 show that the models of Waters and Millero (2013) and Clegg and Whitfield (1995) yield very similar results for these artificial seawater solutions. This is despite the fact that Fig. S4 of the Supporting Information indicates that EMFs of pure aqueous HCl solutions, calculated by the two models, differ by as much as 0.05 mV to 0.1 mV over the ionic strength range of the measurements of Khoo et al. (1977). (A difference of +0.1 mV is equivalent to about -0.0019 in $\ln(\gamma_{HCl})$.) We investigated the reason for this by determining, separately, the contributions of H^+-Cl^- , Na^+-Cl^- , and $H^+-Na^+-Cl^-$ interactions to $\ln(\gamma_{HCl})$ in an acidified artificial seawater solution of 0.7228 mol kg^{-1} ionic strength. The contributions of the H^+-Cl^- interaction were 0.18665 (Waters and Millero model) and 0.18845 (Clegg and Whitfield model), yielding a difference of -0.0018 which is consistent with the difference

found for $\ln(\gamma_{HCl})$ in pure aqueous HCl solutions. The contributions of Na^+-Cl^- interactions to $\ln(\gamma_{HCl})$ in the artificial seawater were very similar for both models, which is also consistent with the result for pure aqueous NaCl (Fig. S5 of the Supporting Information). The values of the $H^+-Na^+-Cl^-$ contribution, from parameters $\theta_{H,Na}$ and $\psi_{H,Na,Cl}$, were found to be 0.0147 (Waters and Millero model) and 0.0128 (Clegg and Whitfield model). These are an order of magnitude smaller than the contribution of the H^+-Cl^- interaction, but the difference of $+0.0019$ between the two almost exactly cancels the difference in the calculated H^+-Cl^- interaction, and explains the very close agreement of the two models shown in Fig. 2.

The values of the parameters for the $H^+-Na^+-Cl^-$ interaction at 25 °C are: $\theta_{H,Na}$ equal to 0.0306 and $\psi_{H,Na,Cl}$ equal to -0.004 (Waters and Millero model, as amended in this work); and $\theta_{H,Na}$ equal to 0.0207 and $\psi_{H,Na,Cl}$ equal to 0.01406 (Clegg and Whitfield model). Both sets of parameters were determined from the EMF measurements of Macaskill et al. (1977), although we retained the original value of $\psi_{H,Na,Cl}$ specified by Waters and Millero model in order to minimize changes. This difference in values demonstrates the dependence of $\theta_{H,Na}$ and $\psi_{H,Na,Cl}$ on the parameters for the cation-anion interactions (here H^+-Cl^- and Na^+-Cl^-) that are used in their determination, and the fact that they need to be consistent in order to obtain the most accurate results.

Although the aspects of the assignment of model parameters noted above are not reflected in the variances and covariances assigned to the parameters in this study, the calculated uncertainty profile in Fig. 3 clearly shows that uncertainties and errors in model-calculated activities are associated with only a few key parameters, and gives indicative values of the magnitudes of those uncertainties. In this particular case – solutions consisting mostly of NaCl, plus lower molalities of $MgCl_2$, $CaCl_2$ and KCl – it was to be expected that the main influences on the HCl activity product would be interactions with Na^+ and Cl^- . However, other solutions are more complex and, in solutions in which multiple equilibria occur, the principal influences and contributors to the uncertainty of calculated speciation and solute activities are more difficult to determine.

5.3. Acidified artificial seawater

The compositions of the artificial seawaters used in the measurements of Khoo et al. (1977), Dickson (1990), and Campbell et al. (1993), are listed in Table 3. The differences between measured and modelled EMFs at 25 °C are shown in Fig. 4, for the Waters and Millero (2013) model. (Results obtained with the Clegg and Whitfield (1995) model are very similar, and are not shown.) The principal uncertainty contributions to the calculated ($E - E^0$) for 0.01 mol kg^{-1} added HCl and salinity 35 are displayed in Fig. 5, and the partial derivatives of the calculated ($E - E^0$) with respect to each parameter are shown in Fig. S2 of the Supporting Information. The main difference in the calculated uncertainties in Fig. 5, compared to the case of the artificial seawater without SO_4^{2-} (Fig. 3), is the large contribution of $\ln(K(HSO_4^-))$ to the total variance. It is likely the greatest in magnitude, given that the contribution of H^+-Cl^- interactions is probably overestimated, for reasons described earlier. There are also a number of interactions involving HSO_4^- and SO_4^{2-} , mainly ternary ones that contribute to the estimated variance at the 0.1% to 1% level. The major contribution of the uncertainty in $\ln(K(HSO_4^-))$ is consistent with the results obtained by Anes et al. (2016).

The interactions Na^+-Cl^- and $H^+-Na^+-Cl^-$ remain important in these solutions, accounting for about 25% of the total estimated variance in the modelled value of ($E - E^0$). Separate calculations of EMFs and uncertainty contributions using the averaged parameter values for those that are unknown yielded results very similar to those shown: the activity of H^+ was lower by 0.03%, and the molality of HSO_4^- greater by 0.05%. The total calculated variance in ($E - E^0$) was increased by less than 0.1%. Interactions between Na^+ and SO_4^{2-} , and Na^+ and HSO_4^- contribute only about 5% to the total calculated variance

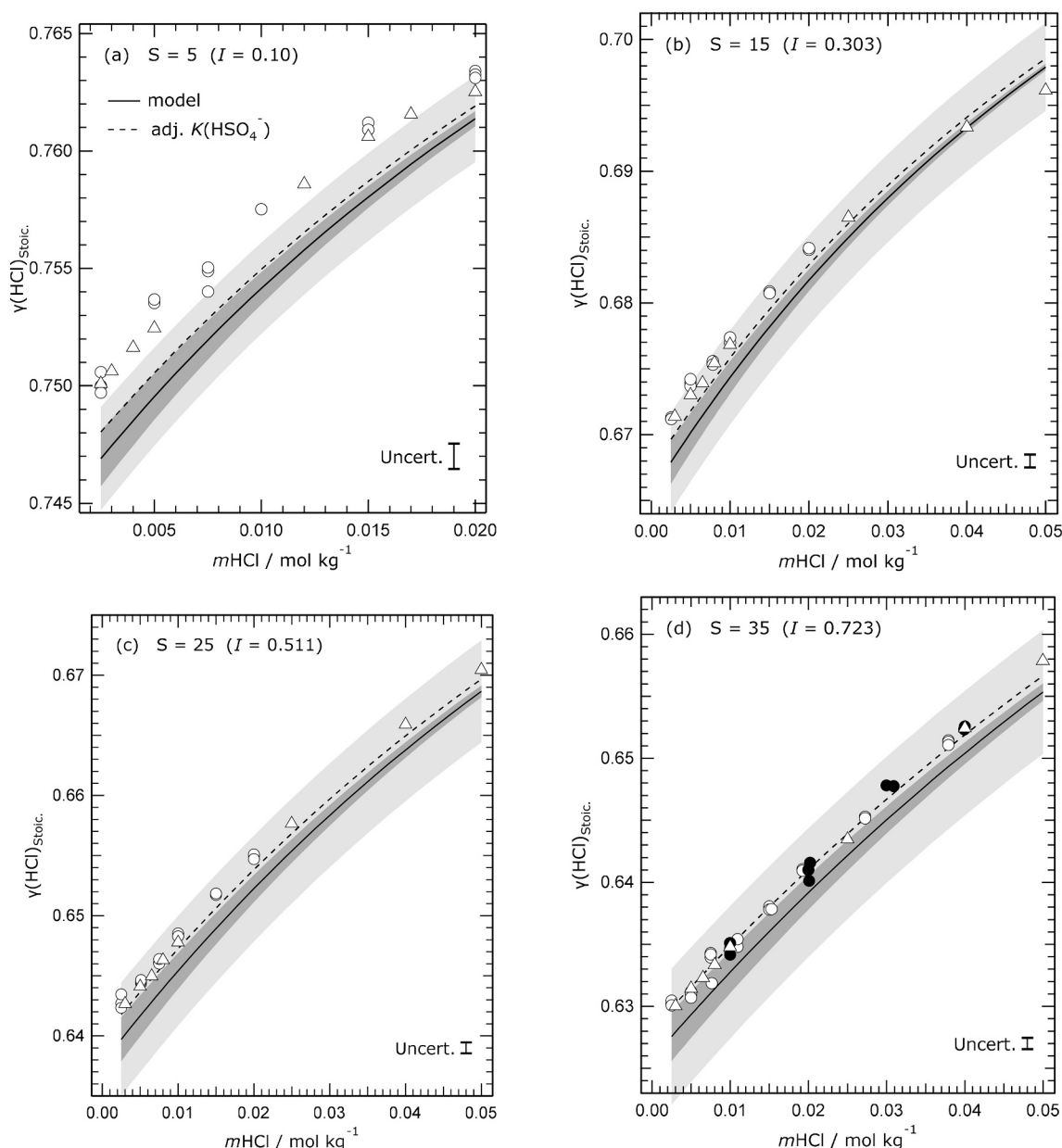


Fig. 6. Stoichiometric mean activity coefficients of HCl ($\gamma(\text{HCl})_{\text{Stoic.}}$) in acidified artificial seawater at 25 °C, plotted against the molality of added HCl ($m\text{HCl}$). Symbols: dot – Khoo et al. (1977); circle – Dickson et al. (1990); triangle – Campbell et al. (1993). Lines: solid – calculated using the model of Waters and Millero (2013); dashed – calculated using the same model but with the adjusted value of $K(\text{HSO}_4^-)$. The lighter shaded area shows the total uncertainty in the calculated values of $\gamma(\text{HCl})_{\text{Stoic.}}$, and the inner (darker) shaded area is the uncertainty attributed to that of the thermodynamic dissociation constant of HSO_4^- . (a) Salinity 5. (b) Salinity 15. (c) Salinity 25. (d) Salinity 35. The estimated uncertainties in the measured $\gamma(\text{HCl})_{\text{Stoic.}}$ (i.e., \pm one standard deviation) are indicated on the plots.

(Fig. 5). We note that, although the $\text{Na}^+ - \text{HSO}_4^-$ interaction is estimated to contribute only 1.36% to the total variance in $(E - E^0)$ compared to 3.6% for $\text{Na}^+ - \text{SO}_4^{2-}$, this may be an underestimate. Aqueous solutions of Na_2SO_4 are comparatively well characterised thermodynamically (e.g., Rard et al., 2000; Holmes and Mesmer, 1986), but the parameters for $\text{Na}^+ - \text{HSO}_4^-$ interactions in the Waters and Millero (2013) model are determined only from osmotic coefficients for aqueous $\text{H}_2\text{SO}_4 - \text{Na}_2\text{SO}_4$ mixtures (Hovey et al., 1993), which must be modelled as the aqueous mixture $\text{H}^+ - \text{Na}^+ - \text{HSO}_4^- - \text{SO}_4^{2-}$. There is no information regarding the sulphate-bisulphate speciation in these solutions, which introduces a greater uncertainty. Also, the Pitzer model of aqueous H_2SO_4 that Hovey et al. used is that of Reardon and Beckie (1987) not Clegg et al. (1994) as adopted by Waters and Millero (2013). Otherwise, most of the contributions are similar to those described in the previous section on artificial seawater without SO_4^{2-} .

The differences between the measured and calculated EMFs (from the Waters and Millero model) in Fig. 4 are mostly negative, and generally lie within the area of model uncertainty. This may be overestimated, for reasons discussed earlier, given that $\text{H}^+ - \text{Cl}^-$ interactions are calculated to make the largest contribution. There is relatively little variation of $\Delta(E - E^0)$ with salinity, and the three datasets plotted agree with each other very well. The uncertainty of the model predictions decreases with salinity, and at a salinity of 5 the calculated EMFs are too high by an average of about 0.2 mV. This exceeds the uncertainty of the experimental measurements, which is indicated on the figure. The consistent negative deviations shown in Fig. 4 were identified by both Waters and Millero (their Fig. 3) and by Clegg and Whitfield (1995) (their Fig. 2).

Fig. 6 shows the same results in terms of the stoichiometric mean activity coefficient of HCl, at four salinities. This quantity, $\gamma_{\text{HCl}(\text{Stoic.})}$, is defined as:

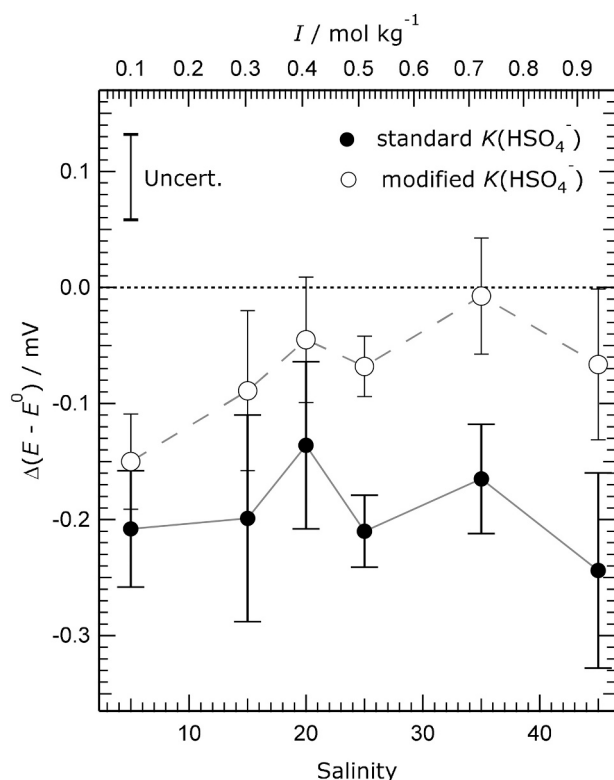


Fig. 7. Mean differences between measured EMFs ($\Delta(E - E^0)$) of acidified artificial seawater at 25 °C, and values calculated using the model of Waters and Millero (2013), at various salinities. The corresponding ionic strengths (I) are shown on the top axis. The errors bars indicate standard deviations. These are the results presented in Table 4. Symbols: dot and solid line – the ‘base case’ model; open circle and dashed line – calculated using the adjusted value of $K(\text{HSO}_4^-)$. The estimated uncertainty in the measured values of $(E - E^0)$ (Uncert.) is indicated on the plot.

$$\gamma_{\text{HCl(Stoic)}} = \gamma_{\text{HCl}} \cdot [m\text{H}^+ / (m\text{H}^+ + m\text{HSO}_4^-)]^{0.5} \quad (9)$$

The deviations of the model from the measured values are generally largest at the lowest added molalities of HCl. The fraction of the total uncertainty in the model calculated values accounted for by $\ln(K(\text{HSO}_4^-))$ is shown as the darker shaded area in both Figs. 4 and 6. Its contribution is greatest at the lowest added molalities of HCl (Fig. 6) because these solutions contain the largest fraction of H^+ present as HSO_4^- (about 10%) and therefore experience the highest sensitivity of free H^+ molality to changes in $K(\text{HSO}_4^-)$. The values of $K(\text{HSO}_4^-)$ used in both models are those determined by Dickson et al. (1990), but adjusted by the addition of 0.03371 in $\ln(K(\text{HSO}_4^-))$ at all temperatures by Clegg et al. (1994) in

order to yield an equilibrium constant of exactly $0.0105 \text{ mol kg}^{-1}$ at 298.15 K, as obtained by Pitzer et al. (1977). The dissociation constant obtained by Dickson et al. (1990) at 298.15 K is $0.01086 \pm 0.0005 \text{ mol kg}^{-1}$ (see Table 1), and it is the uncertainty for this value that has been used in our model calculations.

As a test, we set $K(\text{HSO}_4^-)$ equal to $0.01086 \text{ mol kg}^{-1}$ in the model, and recalculated both $\Delta(E - E^0)$ and $\gamma_{\text{HCl(Stoic.)}}$, see Fig. 7 and the dashed lines in Fig. 6. The changes in $\Delta(E - E^0)$ shown in Fig. 7 are summarised in Table 4. The higher value of $K(\text{HSO}_4^-)$ improves agreement between measured and modelled properties, although the effect is greatest in the higher salinity solutions. The simple change of equilibrium constant ignores the fact that the interaction parameters for $\text{H}^+ - \text{SO}_4^{2-}$ and $\text{H}^+ - \text{HSO}_4^-$ interactions would also be changed in a model of aqueous H_2SO_4 that used this $K(\text{HSO}_4^-)$. However, the uncertainty profile in Fig. 5 shows that the change in just $K(\text{HSO}_4^-)$ should capture the main effect, because uncertainty in the $\text{H}^+ - \text{SO}_4^{2-}$ interaction parameters is estimated to contribute only 0.6% of the total variance. Recent modelling of the thermodynamics of aqueous H_2SO_4 solutions (Sippola and Taskinen, 2014; and references therein) tends to support a value of the dissociation constant greater than $0.0105 \text{ mol kg}^{-1}$, and we conclude that the Pitzer model of aqueous H_2SO_4 should be revised.

6. Comparisons with data from 0 °C to 45 °C

We have evaluated the accuracy of the two models at temperatures other than 25 °C by comparing calculated $(E - E^0)$ with all the measurements of Khoo et al. (1977), Dickson (1990) and Campbell et al. (1993). The results, in Figs. 8 to 11, are plotted as averaged deviations against temperature and various measures of concentration (ionic strength, salinity, and total molality of H^+). No estimates of model uncertainties are shown, because their current treatment is restricted to 25 °C as described earlier.

The results for solutions not containing SO_4^{2-} (from Khoo et al., 1977) are shown in Fig. 8. The plot of mean deviations (for all T) against ionic strength confirms that the pattern of deviations is, on average, the same as at 25 °C (Fig. 2a). The plot of mean deviations against T (for all ionic strengths), Fig. 8b, suggests that deviations of the Clegg and Whitfield (1995) model are positive relative to those of Waters and Millero at the lowest T , and negative at the highest. However, the effect is small. Panel (c) of Fig. 8 compares results at two temperature extremes (5 °C and 40 °C), as measured and calculated γ_{HCl} . The result confirms what is shown in panel (b): the Clegg and Whitfield model yields mean activity coefficients of HCl that are lower than those of Waters and Millero at high temperatures, but the difference is small (about twice the estimated standard uncertainty in the measurements). Both models agree with the data, and with each other, more closely at 5 °C.

The measurements of acidified artificial seawater including SO_4^{2-} by all three groups are compared with the models in Figs. 9 to 11. We note that the data of Campbell et al. (1993) are the most scattered, and the

Table 4

Differences between measured and calculated EMFs (mV) of acidified artificial seawater at 25 °C.

Salinities	Base case ^a	Modified $K(\text{HSO}_4^-)$ ^{a,b}	Base case ^c	Modified $K(\text{HSO}_4^-)$ ^{b,c}
5.0, 5.003	-0.208 ± 0.050 (26)	-0.150 ± 0.041	-0.199 ± 0.052	-0.141 ± 0.042
14.995, 15.0	-0.199 ± 0.089 (25)	-0.089 ± 0.069	-0.192 ± 0.088	-0.082 ± 0.069
20.31	-0.136 ± 0.072 (9)	-0.045 ± 0.054	-0.135 ± 0.073	-0.045 ± 0.055
25	-0.210 ± 0.031 (26)	-0.068 ± 0.026	-0.215 ± 0.031	-0.074 ± 0.026
34.99, 35.0	-0.165 ± 0.047 (44)	-0.073 ± 0.050	-0.180 ± 0.048	-0.022 ± 0.049
44.55, 45.0	-0.244 ± 0.084 (34)	-0.066 ± 0.065	-0.260 ± 0.092	-0.082 ± 0.071

Notes: The data of Dickson (1990), Khoo et al. (1977), and Campbell et al. (1993) are used. The values tabulated are the mean differences between measured and calculated $(E - E^0)$ (in mV) at each salinity. See also Fig. 7.

^a The calculations were carried out using the Waters and Millero (2013) model. The numbers of measurements at each salinity are given in parentheses. These results correspond to those plotted, for the individual measurements, in Fig. 4.

^b For these calculations the value of $K(\text{HSO}_4^-)$ at 25 °C was increased in the model from $0.0105 \text{ mol kg}^{-1}$ to $0.01086 \text{ mol kg}^{-1}$ (from the fitted equation of Dickson et al., 1990).

^c The calculations were carried out using the Clegg and Whitfield (1995) model.

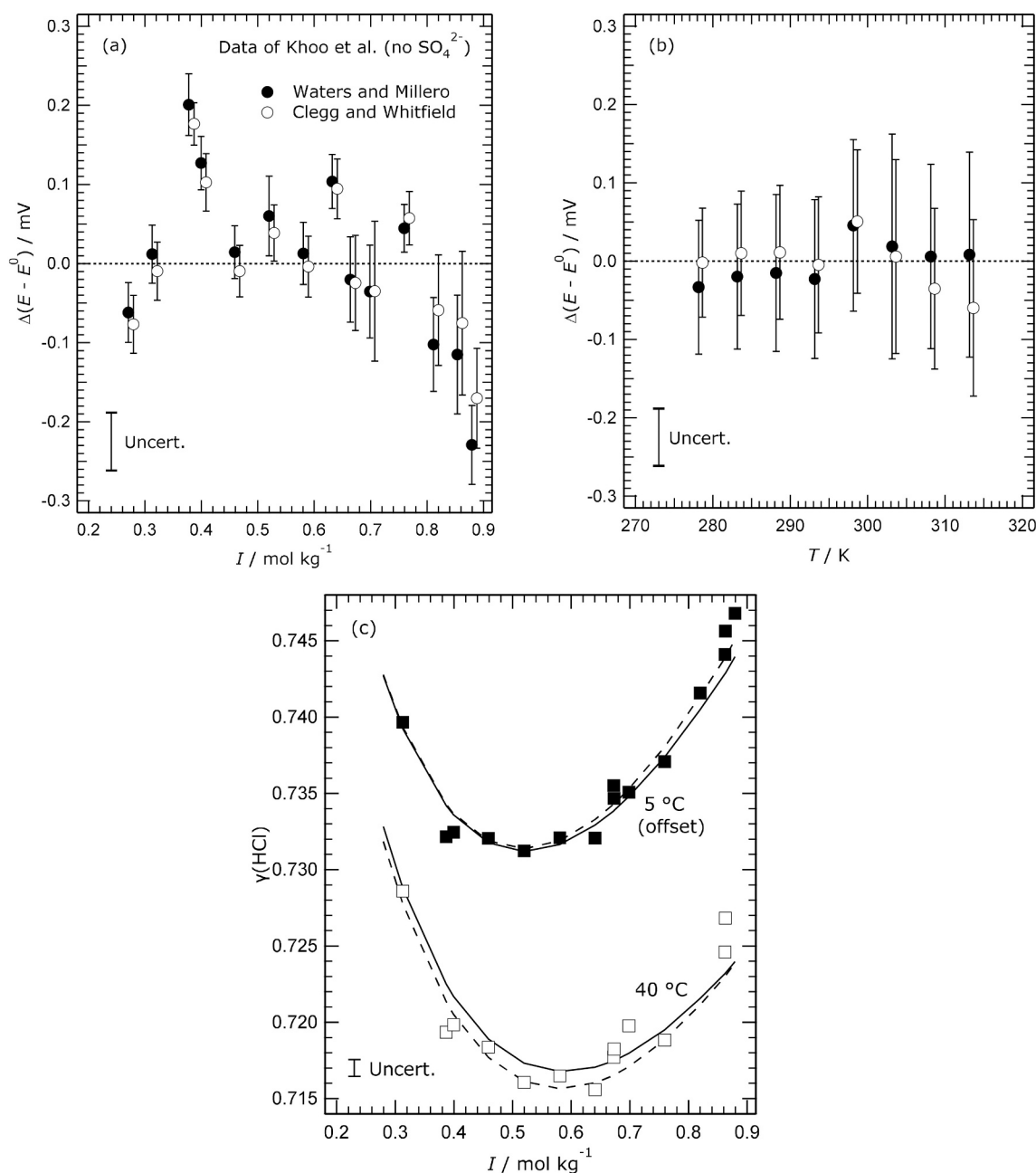


Fig. 8. Comparison of measured EMFs of acidified artificial seawater (without SO_4^{2-}) with values calculated using the models of Waters and Millero (2013) and Clegg and Whitfield (1995). The data are from Khoo et al. (1977). (a) Mean differences between measured and calculated EMFs ($\Delta(E - E^0)$) for all temperatures (278.15 to 313.15 K), plotted against ionic strength (I). The bars indicate the standard deviations. Symbols: dot – Waters and Millero (2013) model; open circle – Clegg and Whitfield (1995) model. (b) Mean differences at individual temperatures (T) for all ionic strengths. The meanings of the symbols and bars are the same as in (a). Note that the results for the Clegg and Whitfield (1995) model are offset to the right of those of Waters and Millero (2013) in plots (a) and (b) to aid legibility. The estimated uncertainty in the measured ($E - E^0$) (i.e., \pm one standard deviation) is indicated. (c) Mean activity coefficients of HCl (γ_{HCl}) at two temperatures, calculated from the EMF measurements. Symbols: solid square – 5 °C; open square – 40 °C. Lines: solid – model of Waters and Millero; dashed – model of Clegg and Whitfield. All values of γ_{HCl} at 5 °C are reduced by 0.06 to improve legibility.

final two rows of their results (section (e) of their Appendix 1), and some other individual points, were omitted from our analysis. The most important single feature of our comparisons is that the consistent negative deviation in ($E - E^0$) of about -0.1 mV to -0.2 mV, found at 25 °C (Fig. 4), also occurs at all other temperatures (panels (b) of Figs. 9 to 11). This deviation does not appear to vary much with temperature. It is further evidence that the value of the thermodynamic equilibrium constant $K(\text{HSO}_4^-)$ and the Pitzer model of aqueous H_2SO_4 of which it is a part, should be revised.

Mean deviations in ($E - E^0$) at different salinities, shown in panels (a)

of Figs. 10 and 11, do not appear to show any consistent variation. However, the mean deviations for salinity 35 and for different added molalities of HCl (Fig. 9a, and panels (c) of Figs. 10 and 11) become less at higher $m\text{HCl}$ relative to the average of about -0.2 mV. The reason for this small effect is not clear, although it may be related to the greater reduction in $m\text{SO}_4^{2-}$, the molality of free sulphate, in the more acid solutions.

The trend of the two models with temperature, relative to one another, for acidified artificial seawater including SO_4^{2-} is shown in Figs. 9 to 11 (panels (b)). All three datasets show qualitatively the same

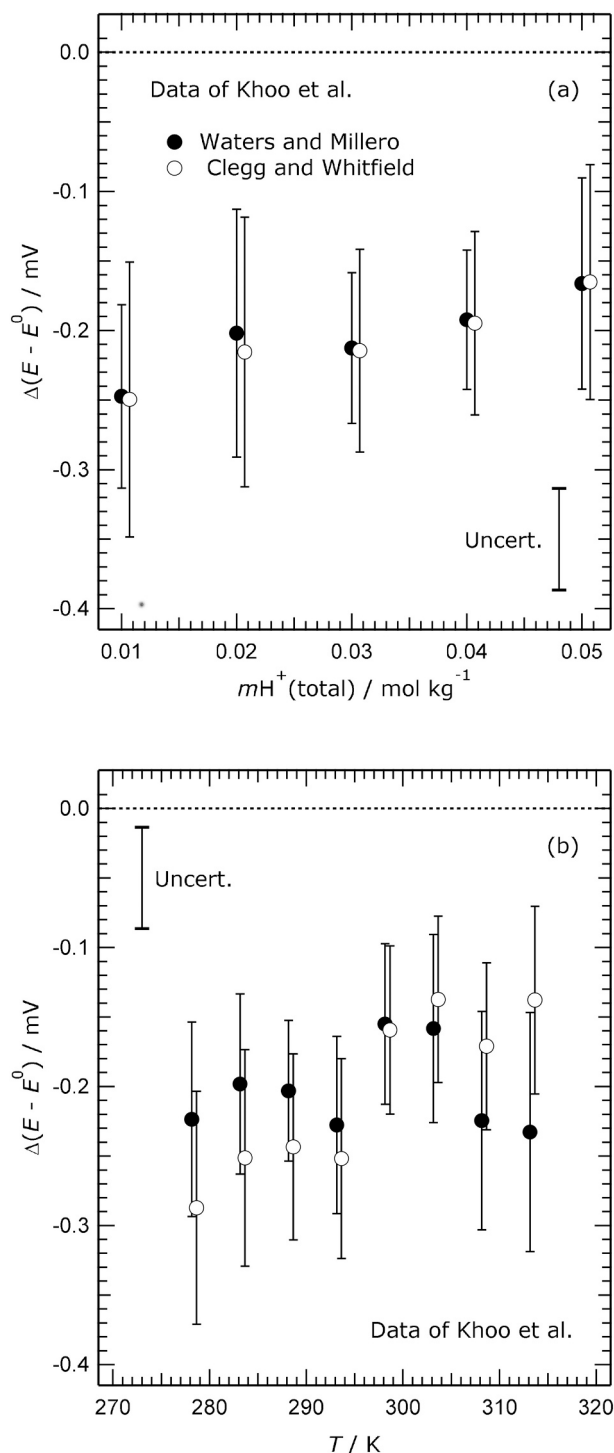


Fig. 9. Comparison of measured EMFs of acidified artificial seawater with values calculated using the models of Waters and Millero (2013) and Clegg and Whitfield (1995). The data are from Khoo et al. (1977). (a) Mean differences between measured and calculated EMFs $\Delta(E - E^0)$ at individual molalities of total H^+ ($mH^+(\text{total})$) for all temperatures (278.15 to 313.15 K) and salinities (20.31, 34.99, and 44.55). The bars indicate the standard deviations. Symbols: dot – Waters and Millero (2013) model; open circle – Clegg and Whitfield (1995) model. (b) Mean differences at individual temperatures (T) for all salinities and total H^+ ion molalities (0.009948 to 0.05041 mol kg^{-1}). The meanings of the symbols and bars are the same as in (a). The results for the Clegg and Whitfield (1995) model are offset to the right of those of Waters and Millero (2013) in both plots to aid legibility. The estimated uncertainty in the measured $(E - E^0)$ (i.e., \pm one standard deviation) is indicated on the plots.

result: the differences between the models are very small at 25 °C, but the model of Clegg and Whitfield yields negative deviations in $(E - E^0)$ relative to the model of Waters and Millero at lower T , and positive deviations at higher T . Given that the values of $K(HSO_4^-)$, and the H^+ - SO_4^{2-} and H^+ - HSO_4^- interaction parameters, are the same in both models it is likely that the cause is one of the principal ion interactions affecting calculated EMF (Fig. 5) for which different sets of parameters are used. This is the case for both H^+ - Cl^- and Na^+ - Cl^- interactions.

The comparisons of the models and measurements in terms of γ_{HCl} , at 0 and 40 °C and salinity 35 (panels (d) of Figs. 10 and 11) confirm what is shown in the plots of mean $\Delta(E - E^0)$ against temperature in the same figures: the model of Clegg and Whitfield yields lower γ_{HCl} than that of Waters and Millero at 0 °C, and this difference is reversed at 40 °C.

7. Calculation of the standard EMF, E^* , of the total pH scale

The total pH scale (pH_T) is calibrated from Harned cell measurements of equimolar $TrisH^+$ and $Tris$ in solutions of artificial seawater (DelValls and Dickson, 1998), combined with a standard cell potential, E^* , determined from measurements of acidified artificial seawater extrapolated to zero added HCl (Dickson, 1990, see his eq. 14). A direct calculation of E^* using the speciation models can, in principle, be used to quantify the uncertainties involved in its empirical determination. It can also contribute to the definition of pH on the total scale for natural waters of non-seawater stoichiometry because the model can calculate E^* for solutions of arbitrary composition. In this section we examine the use of the model to estimate E^* .

First, a stoichiometric hydrogen ion molality defined as the sum of the free hydrogen ion molality (mH^+) and bisulphate molality ($mHSO_4^-$) can be written:

$$mH^+ + mHSO_4^- = mH^+ (1 + mSO_4^{2-} / K^*(HSO_4^-)) \quad (10)$$

where mSO_4^{2-} is the molality of the free sulphate in solution, and $K^*(HSO_4^-)$ is the stoichiometric dissociation constant of the bisulphate ion given by:

$$K^*(HSO_4^-) = K(HSO_4^-) \cdot (\gamma_{HSO_4^-} / \gamma_{H^+} \gamma_{SO_4^{2-}}) \quad (11)$$

In this equation $K(HSO_4^-)$ is the thermodynamic value of the dissociation constant at the temperature of interest, and the three activity coefficients all vary with temperature and the composition of the solution.

The standard expression for the EMF of a Harned cell containing any solution including H^+ and Cl^- ions can be expressed in terms of the stoichiometric hydrogen ion molality as follows:

$$E = \left\{ E^0 - (RT/F) \cdot [2 \ln(\gamma_{HCl}) - \ln(1 + mSO_4^{2-} / K^*(HSO_4^-))] \right\} - (RT/F) \cdot \ln((mH^+ + mHSO_4^-) \cdot mCl^-) \quad (12)$$

where γ_{HCl} is the mean activity coefficient of HCl in the solution. Note that, if Eq. (12) is applied to solutions not containing SO_4^{2-} , then $mHSO_4^-$ and the logarithmic term on the first line containing mSO_4^{2-} will both be zero. For a solution of artificial seawater containing trace added HCl the quantity in $\{\}$ in Eq. (12) is equivalent to a standard potential of the cell E^* (V) for the temperature and salinity of interest, and is obtained experimentally by the extrapolation of measured EMFs to zero HCl molality (Dickson, 1990). The standard potential is given by:

$$E^* = E^0 - (RT/F) \cdot [2 \ln(\gamma_{HCl}^{(tr)}) - \ln(1 + mSO_4^{2-(T)} / K^*(HSO_4^{-(tr)}))] \quad (13)$$

where the superscript (tr) means that the value is for trace (zero) HCl in artificial seawater. In such a solution the molality of HSO_4^- is so small relative to that of SO_4^{2-} that the total SO_4^{2-} molality, denoted by superscript (T), can be used without loss of accuracy. This definition is Eq. (13) of Dickson (1990).

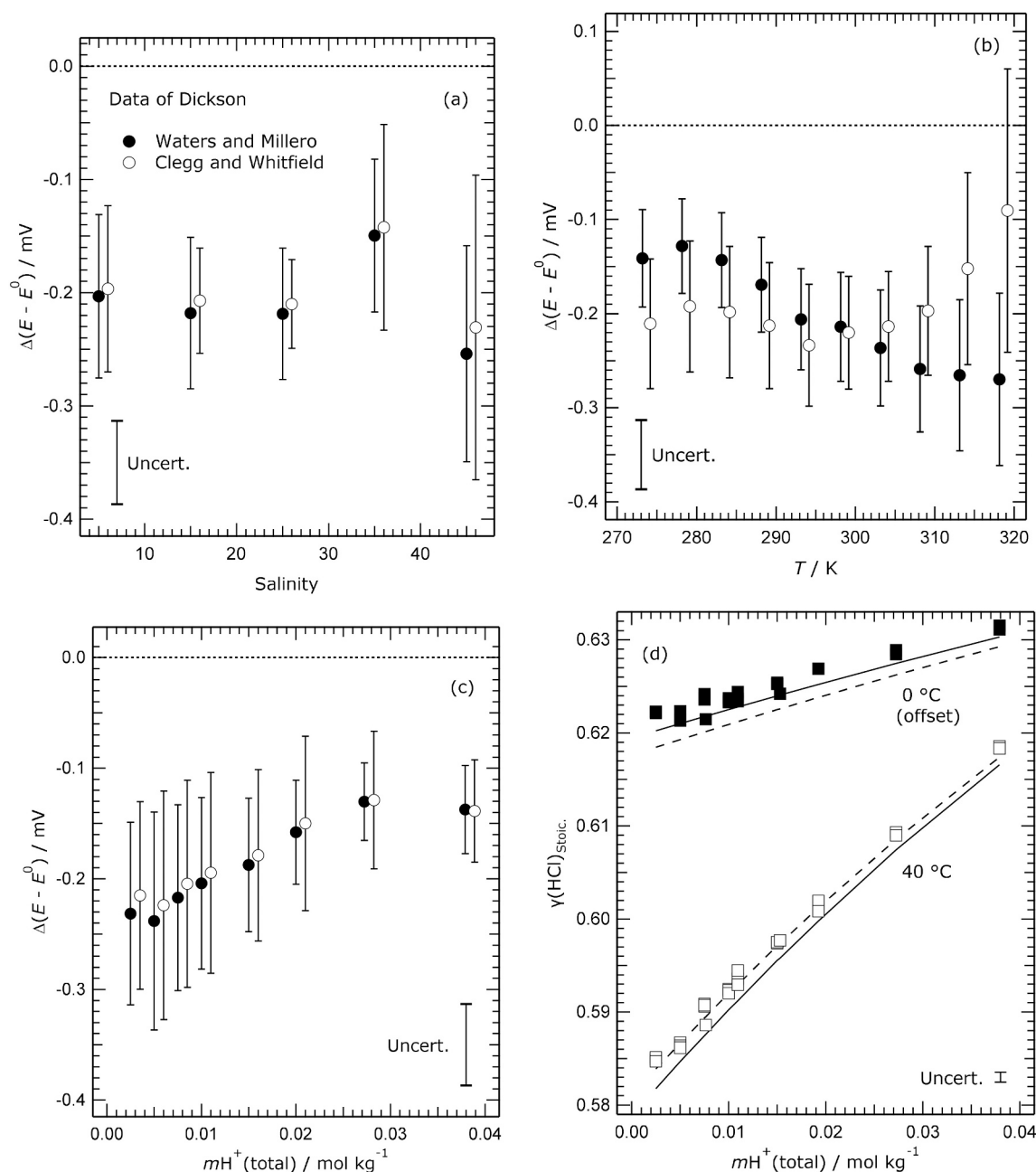


Fig. 10. Comparison of measured EMFs (and γ_{HCl} derived from them) of acidified artificial seawater with values calculated using the models of Waters and Millero (2013) and Clegg and Whitfield (1995). The data are from Dickson (1990). (a) Mean differences between measured and calculated EMFs ($\Delta(E - E^0)$) as a function of salinity for all temperatures (273.15 to 318.15 K) and total H^+ ion molalities (0.0025 to 0.0379 mol kg^{-1}). The bars indicate the standard deviations. Symbols: dot – Waters and Millero (2013) model; open circle – Clegg and Whitfield (1995) model. (b) Mean differences at individual temperatures (T) for all salinities (5 to 45) and total H^+ ion molalities. (c) Mean differences at individual values of $mH^+(total)$ for all salinities (5 to 45) and all temperatures. The meanings of the symbols and bars in plots (b) and (c) are the same as in (a). The results for the Clegg and Whitfield (1995) model are offset to the right of those of Waters and Millero (2013) in these plots to aid legibility. (d) Measured and calculated γ_{HCl} at two temperatures, and salinity 35, plotted against total H^+ ion molality ($mH^+(total)$). Symbols: solid square – 0 °C (0.06 has been subtracted from all values); open square – 40 °C. Lines: solid – model of Waters and Millero (2013); dashed – model of Clegg and Whitfield (1995). The estimated uncertainties in the measured γ variable (i.e., \pm one standard deviation) are indicated on the plots.

The uncertainty profile for E^* , calculated using the model of Waters and Millero (2013) for salinity 35, is shown in Fig. 12. It is very similar to that of the EMF of acidified artificial seawater (Fig. 5): the uncertainty contribution of $\ln(K(HSO_4^-))$ is greatest (38% of the total variance), together with that of the H^+-Cl^- interaction. This is followed by Na^+-Cl^- (about 14%), and then ternary interactions of $H^+-Na^+-Cl^-$. Other contributions are at the 5% level and below. The estimated standard deviation in E^* , 0.45 mV, is close to that of the calculated EMFs of acidified artificial seawater of this salinity (Fig. 4). Waters and Millero (2013)

have shown that the datasets of Khoo et al. (1977), Dickson (1990), and Campbell et al. (1993) yield values of E^* that are consistent to within about 0.1 mV. This is much smaller than the estimated standard deviation in E^* calculated directly by the model. The contribution of H^+-Cl^- interactions to this uncertainty (about 26% of the variance) may be too high by a factor of 2 or more, so that the true standard deviation is somewhat smaller. Obtaining a more accurate value than is currently used in the models – and reducing its uncertainty – is essential and appears to be the key to a more accurate prediction of E^* , as it is for the

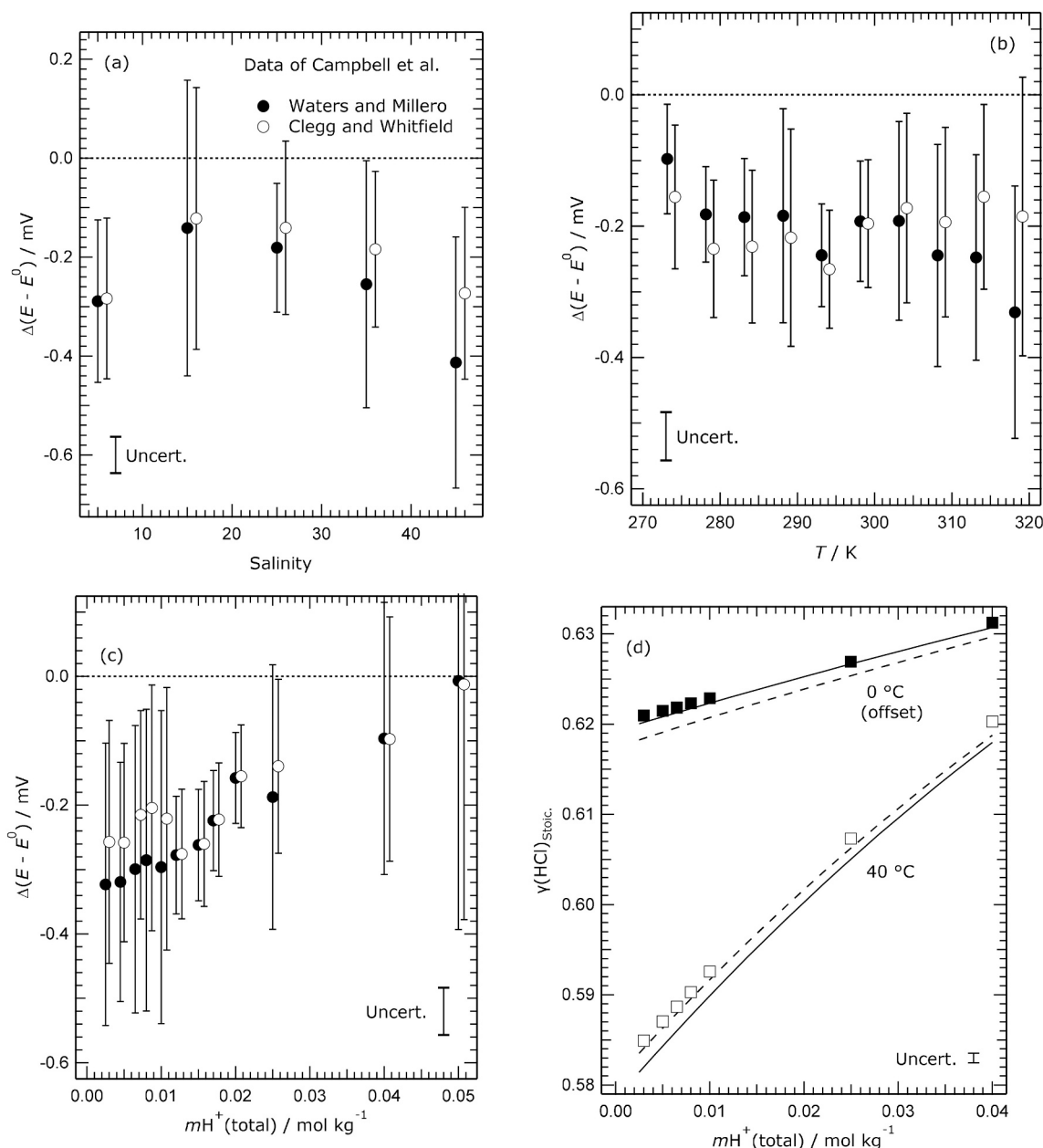


Fig. 11. Comparison of measured EMFs (and γ_{HCl} derived from them) of acidified artificial seawater with values calculated using the models of Waters and Millero (2013) and Clegg and Whitfield (1995). The data are from Campbell et al. (1993). The meanings of the symbols and lines in all plots (a) to (d) are the same as those in Fig. 10.

EMFs of the acidified seawaters generally. This is examined further below.

Dickson (1990) obtained values of E^* empirically, by fitting the following quadratic equation:

$$E + (RT/F) \cdot \ln(m\text{HCl} \cdot m\text{Cl}^-) = b_0 + b_1 \cdot m\text{HCl} + b_2 \cdot m\text{HCl}^2 \quad (14)$$

where E (V) is the measured EMF, $m\text{HCl}$ is the molality of added HCl in the solution, $m\text{Cl}^-$ is the total chloride molality, and b_{0-2} are the fitted coefficients. The coefficient b_0 is equivalent to E^* , for which values are listed in Table 3 of Dickson (1990). The fits of the data, for salinity 35 and temperatures 25 °C and 5 °C, are reproduced in Fig. 13 where the plotted quantity E^* is the left hand side of Eq. (14) above. The solid lines show the model predictions, using the standard $K(\text{HSO}_4^-)$ value in the speciation models (i.e., as given by Clegg et al., 1994). The predicted values are high by about 0.2 mV, corresponding to the results shown in

Fig. 7, and 6d. However, the use of values of $K(\text{HSO}_4^-)$ from the study of Dickson et al. (1990) (dashed lines in Fig. 13) yields predicted E^* in excellent agreement with both the measurements and the empirical fits. The E^* calculated using the model differ from the directly fitted values (b_0) by <0.01 mV, which is less than the uncertainty in the measurements.

We conclude that, first, the results in general confirm that the empirical fit of Eq. (14) yields satisfactory estimates of E^* , and that the uncertainty is dominated by that of the measurements themselves and not artifacts of the fitting procedure. Second, the very close agreement of the model with the data, although not yet attained at other salinities, gives encouragement that an accurate model of this chemical system is achievable. Third, such a model should include a new Pitzer model parameterisation of the aqueous H_2SO_4 (including revised values of $K(\text{HSO}_4^-)$).

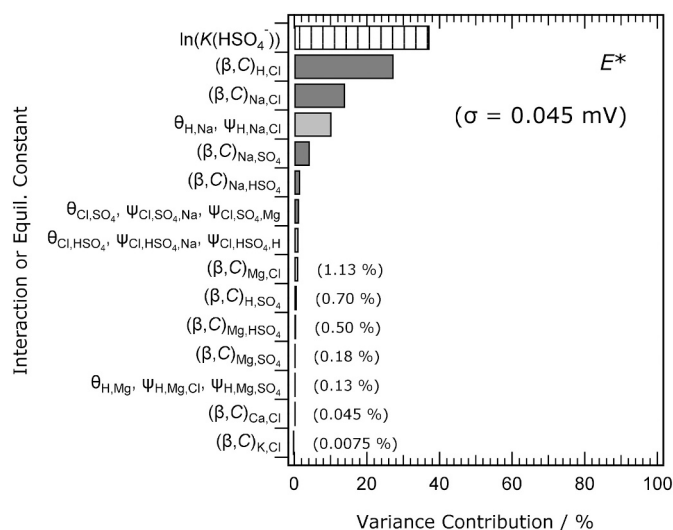


Fig. 12. Percentage contributions of individual Pitzer model interactions, and equilibrium constants, to the variance of the calculated E^* (Eq. (13)) at 25 °C of a Harned cell containing artificial seawater of salinity 35. The parameters associated with each of the interactions are listed down the left hand side, and contributions of about 1% and below are noted on the plot. Interactions with very small variance contributions (below 0.0075%) are omitted. The predicted standard deviation (σ) is 0.045 mV.

8. Recommendations for future work

Here we summarise new measurements and reassessments of existing data that are needed to improve the models of artificial seawater at all temperatures, with the aim of achieving agreement with measured EMFs to within, or close to, experimental uncertainty. This is needed both for applications in the definition and determination of pH, and as the basis for a larger model of speciation in natural waters. The profiles in Figs. 3, 5, and 12 identify the major contributors to the uncertainty of model predictions of EMF and E^* at 25 °C, and therefore those interactions and equilibrium constants that must be calculated most accurately in a successful model. These are identified in Table 5, together with the predicted quantities for which they are most important. There are two general points to bear in mind. First, improved agreement between measured and modelled EMFs requires the calculation of activities and activity coefficients to better than 1% accuracy. This is likely to require that the key ternary mixture parameters – notably $\theta_{H,Na}$ and $\psi_{H,Na,Cl}$ for $H^+-Na^+-Cl^-$ interactions, but also interactions for other ions – should always be determined using the same parameters for the cation-anion binary interactions ($\beta_{ca}^{(1-2)}$, $C_{ca}^{(0,1)}$) as are used in the models. Second, the analysis in this study is primarily for the single temperature of 25 °C, and there are a number of solute interactions that have only been quantified at this temperature. The use of these parameters in calculations for other temperatures will result in larger errors and uncertainties than would be expected from their positions in the uncertainty profiles. This is apparent in the larger standard deviations, and poorer agreement between models and data shown at the temperature extremes (see panels (b) of Figs. 9 to 11)). The parameters can be identified in the tables in the Supplementary Information, and those likely to be most significant are included in Table 5. The contents of the table are discussed below.

8.1. Aqueous HCl, and $H^+-Na^+-Cl^-$ solutions

The parameter $\theta_{H,Na}$ in the Waters and Millero (2013) model has been revised in this work as noted earlier, by fitting to EMFs of $H^+-Na^+-Cl^-$ aqueous solutions measured by Macaskill et al. (1977). These data were also used by Clegg and Whitfield (1995). The deviations between measured and fitted EMFs, for the lowest molalities of HCl in

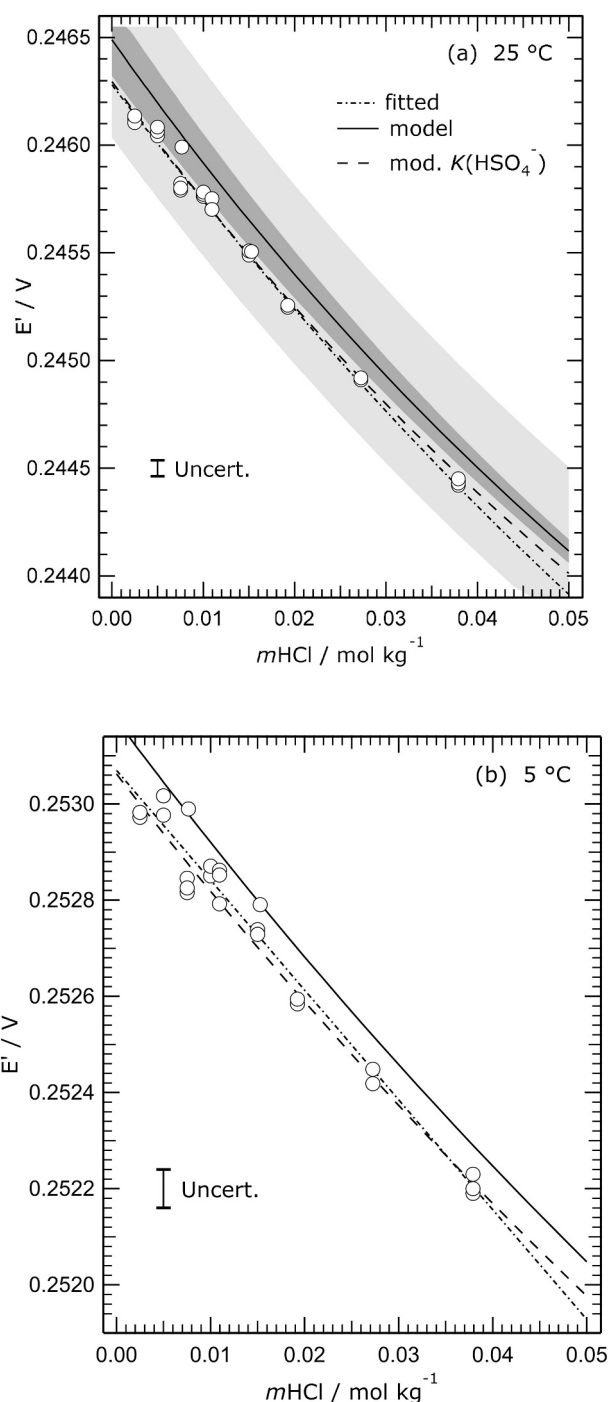


Fig. 13. Measured and calculated E^* (Eq. (14)) in salinity 35 seawater, plotted against the total molality of added HCl ($mHCl$). Symbols: measurements of Dickson (1990). Lines: solid – calculated using the model of Waters and Millero (2013); dashed – calculated using the same model but with the modified value of $K(HSO_4^-)$; dash-dot – fitted to the measurements, using Eq. (14) of Dickson (1990). The lighter shaded area shows the total uncertainty in the calculated values of E^* , and the inner (darker) shaded area is the uncertainty attributed to that of the thermodynamic dissociation constant of HSO_4^- . (a) 25 °C. (b) 5 °C.

the mixtures, range from -0.1 to $+0.06$ mV at 25 °C for the Waters and Millero model. The corresponding ranges for the model of Clegg and Whitfield are -0.05 mV to $+0.02$ mV. The pattern of deviations in $(E - E^0)$, with respect to $mHCl$ in the mixtures, differs between the two models. We recommend that both $\theta_{H,Na}$ and $\psi_{H,Na,Cl}$ parameters be

Table 5

Interactions and equilibrium constants that need reassessment.

Solutions	Parameters or equilibrium constants	T	ASW (no SO_4^{2-})	ASW	Notes
HCl	$\beta^{(0,1)}_{\text{H,Cl}}, C^{(0,1)}_{\text{H,Cl}}$	f(T)	$\underline{\text{X}}$	$\underline{\text{X}}$	a
HCl/NaCl	$\theta_{\text{H,Na}}, \psi_{\text{H,Na,Cl}}$	f(T)	$\underline{\text{X}}$	$\underline{\text{X}}$	a
acid sulphate mixtures	$K(\text{HSO}_4^-)$	f(T)	$\underline{\text{X}}$	$\underline{\text{X}}$	b
Other Interactions ^c					
NaCl	$\beta^{(0,1)}_{\text{Na,Cl}}, C^{(0,1)}_{\text{Na,Cl}}$	f(T)		x	d
$\text{H}^+ \text{-Na}^+ \text{-SO}_4^{2-}$	$\beta^{(0,1)}_{\text{Na,HSO}_4}, C^{(0,1)}_{\text{Na,HSO}_4}$	25 °C		$\underline{\text{X}}$	e
acid $\text{SO}_4^{2-}/\text{Cl}^-$ mixtures	$\theta_{\text{Cl,SO}_4}, \theta_{\text{Cl,HSO}_4}$	25 °C		x	f
$\text{H}^+ \text{-Mg}^{2+} \text{-SO}_4^{2-}$	$\beta^{(0,1)}_{\text{Mg,HSO}_4}, C^{(0,1)}_{\text{Mg,HSO}_4}$	25 °C		x	g

Notes: this table lists the parameters and equilibrium constants that are the main contributors to the uncertainties of calculated EMFs of the indicated mixtures. The most significant are indicated by 'X', and those that contribute slightly less by 'x'. The entry in the temperature column ('T') indicates whether the existing parameters or equilibrium constants are for the single temperature of 25 °C, or over a range of temperatures ('f(T)') in the model of Waters and Millero (2013). Cases for which the model of Clegg and Whitfield (1995) differs are indicated in the notes below. The abbreviation ASW means acidified artificial seawater.

^a The parameters for both $\text{H}^+ \text{-Cl}^-$ and $\text{H}^+ \text{-Na}^+ \text{-Cl}^-$ interactions should be reassessed together from the extensive data in the literature.

^b A number of alternative sets of equilibrium constants are available, as elements of thermodynamic models of $\text{H}_2\text{SO}_{4(\text{aq})}$, for example: Clegg et al. (1994); Knopf et al. (2003); Sippola and Taskinen (2014).

^c Other interactions, for which the partial derivative of the indicated EMF with respect to the parameter is at a level of 20% of more of the highest value.

^d The Pitzer model from the critical review of Archer (1992), and later work by Archer and Carter (2000), is a likely alternative to the parameters used by Waters and Millero (2013).

^e These parameters are from isopiestic measurements of water activity (in the model of Clegg and Whitfield they vary with temperature).

^f The existing values in the model of Waters and Millero are from isopiestic ($\theta_{\text{Cl,SO}_4}$, Wu et al. (1968)) and EMF ($\theta_{\text{Cl,HSO}_4}$, Storonkin et al. (1967) measurements). In the model of Clegg and Whitfield parameter $\theta_{\text{Cl,SO}_4}$ varies with temperature.

^g The values of these parameters in the Waters and Millero model are from isopiestic measurements (Rard and Clegg, 1999) and those in the Clegg and Whitfield model (obtained by Harvie et al., 1984) are from EMF measurements yielding stoichiometric mean activity coefficients of H_2SO_4 (Harned and Sturgis, 1925). In addition, Clegg and Whitfield assumed that the parameters had the same temperature coefficients as those of $\text{Mg}(\text{ClO}_4)_2$.

revised, based on a larger set of available measurements. There are numerous sources of early data cited by Harned (1959), the work of Hawkins (1932) at 25 °C for 4 mol kg^{-1} to 6 mol kg^{-1} ionic strength solutions, and the study of Macaskill et al. (1977) already mentioned. The work of White et al. (1980), who have measured EMFs of $\text{H}^+ \text{-Na}^+ \text{-Mg}^{2+} \text{-Cl}^-$ solutions, is also relevant. If the accuracy with which EMFs of $\text{H}^+ \text{-Na}^+ \text{-Cl}^-$ solutions can be reproduced is limited by the model-calculated interactions for aqueous HCl, as appears possible from our calculations, then revisions could be carried out using sources of data cited by Hamer and Wu (1972), Carslaw et al. (1995), and Partanen et al. (2007) for aqueous HCl.

Interactions for $\text{Na}^+ \text{-Cl}^-$ are also noted in the lower section of Table 5. The uncertainty profile for EMFs of acidified artificial seawater (Fig. 5) shows that $\text{Na}^+ \text{-Cl}^-$ interactions have about the same contribution as those for $\text{H}^+ \text{-Na}^+ \text{-Cl}^-$ (and about a half that of $\text{H}^+ \text{-Cl}^-$). A revision of the model of Waters and Millero to include parameters from the critical review of Archer (1992) should be investigated. We note that there are small differences between the osmotic and activity coefficients of Archer (1992) and those from Clarke and Glew (1985) (Fig. S5 of the Supporting Information), but it is unclear what significance they might have for the calculation of natural water properties. Clarke and Glew (1985) used an equation similar to that of Pitzer (with parameters equivalent to $\beta^{(0)}_{\text{Na,Cl}}$, $\beta^{(1)}_{\text{Na,Cl}}$, and $C^{(0)}_{\text{Na,Cl}}$) but extended with two further terms.

8.2. The dissociation constant of HSO_4^-

Calculated EMFs of acidified artificial seawater are consistently higher than measured (Fig. 4) and it appears that the value of $K(\text{HSO}_4^-)$ in the model – which was fixed to the value at 25 °C obtained by Pitzer et al. (1977) – is too low. An increase of 3.4%, to agree with the value determined by Dickson et al. (1990) (their fitted equation), has been shown in Figs. 6, 7 and 13 to yield an improvement. Nair and Nancollas (1958) obtained a value of 0.0109 mol kg^{-1} for $K(\text{HSO}_4^-)$ at 25 °C from their EMF measurements of low ionic strength HCl- H_2SO_4 aqueous solutions. This value is essentially the same as that obtained by Dickson et al. (1990). There does not appear to be an experiment able to

determine $K(\text{HSO}_4^-)$ unambiguously, and a satisfactory speciation model of aqueous H_2SO_4 thermodynamic properties can be obtained based upon a range of different $K(\text{HSO}_4^-)$ (Pitzer et al., 1977; Sippola, 2013). The model of Clegg et al. (1994) for aqueous H_2SO_4 should be rederived, based upon higher values of $K(\text{HSO}_4^-)$, and including both new data that have become available since their study and some older work that was overlooked. These data include osmotic coefficients, EMFs of two electrochemical cells, and heats of dilution (J. A. Rard, pers. comm.). It is recommended that the values of $K(\text{HSO}_4^-)$ obtained by Dickson et al. (1990) are used. We note that the model of Sippola and Taskinen (2014) used $K(\text{HSO}_4^-)$ equal to 0.0119 mol kg^{-1} at 25 °C. However, the values of the dissociation constant were determined as a part of the fit of the overall model in their study, rather than being determined separately, and their model did not include some enthalpy measurements or any heat capacity measurements as a part of the fitted dataset. Both types of data can be used to quantify the variation of solvent and solute activities with temperature (e.g., Pitzer, 1991).

8.3. Other interactions

The parameters and solutions listed under this heading in Table 5, with the exception of NaCl, are specified only at 25 °C in the model of Waters and Millero (2013). (In the model of Clegg and Whitfield (1995) both $\theta_{\text{Cl,SO}_4}$ and the parameters for $\text{Na}^+ \text{-HSO}_4^-$ interactions vary with T, but newer data have become available.) Consequently the uncertainty profiles for EMFs and E^* are not likely to represent accurately the contributions of this group of parameters to the overall uncertainty for other temperatures. The contributions are likely to be larger.

The two mixture parameters $\theta_{\text{Cl,SO}_4}$ and $\theta_{\text{Cl,HSO}_4}$ are generally determined in combination with the parameters $\psi_{\text{Cl,SO}_4,c}$ and $\psi_{\text{Cl,HSO}_4,c}$ respectively (where c is H^+ or a major seawater cation such as Na^+ or Mg^{2+}). The value of $\theta_{\text{Cl,SO}_4}$ equal to 0.020 at 25 °C in both models (Harvie and Weare, 1980; Pitzer and Kim, 1974) is based upon isopiestic measurements of Wu et al. (1968). Rard et al. (2003), using a larger range of data (and different cation-anion parameters for $\text{Na}^+ \text{-Cl}^-$ and $\text{Na}^+ \text{-SO}_4^{2-}$ interactions), obtained a lower value of 0.0124 ± 0.00033 at 25 °C and also determined the variation of $\theta_{\text{Cl,SO}_4}$ with temperature.

Friese and Ebel (2010) list numerous sources of thermodynamic measurements for the NaCl-Na₂SO₄ aqueous solutions, covering a range of temperatures. There appear to be sufficient data in the literature to re-evaluate this parameter at all temperatures of interest.

The Na⁺-HSO₄⁻ interaction parameters in the model of Waters and Millero (2013) come from the study of Hovey et al. (1993), and are based upon the isopiestic measurements at 25 °C of Na₂SO₄-H₂SO₄ aqueous solutions by Rard (1989, 1992). The mixture parameters determined by Hovey et al. for this system were not adopted by Waters and Millero. Values of the Na⁺-HSO₄⁻ interaction parameters in the model of Clegg and Whitfield (1995) are based upon the same isopiestic data, and also EMF measurements (see their section 4.1), and their treatment is self-consistent. In their model the variation of the Na⁺-HSO₄⁻ parameters with temperature was obtained by analogy, from fitted enthalpies of aqueous NaClO₄. The EMF measurements of Pierrot et al. (1997), of aqueous HCl-Na₂SO₄ solutions from 0 to 50 °C, are also relevant. The model of H⁺-Na⁺-Cl⁻-HSO₄⁻-SO₄²⁻ solutions should be revised, using all of the available data, to obtain the values of the Na⁺-HSO₄⁻ parameters as functions of temperature.

The interactions of Mg²⁺ with HSO₄⁻ ions in the two models were determined from different datasets (see the notes to Table 5), both for 25 °C. Measurements of EMFs of HCl-MgSO₄ aqueous mixtures have since been made from 5 to 45 °C by Lu et al. (2005), and improved values of parameters for Mg²⁺-HSO₄⁻ should be determinable, as a function of temperature, from the combined data.

The value of $\theta_{\text{Cl,HSO}_4}$ in both models (from Harvie et al., 1984) appears to be based upon the EMFs of aqueous mixtures at 25 °C measured by Storonkin et al. (1967). In contrast, Pierrot et al. (1997) found that $\theta_{\text{Cl,HSO}_4}$ could be set to zero at all temperatures. It may be possible to determine whether this parameter is indeed redundant from the EMF measurements of HCl-MgSO₄ aqueous mixtures noted above.

The interactions for H⁺-Mg²⁺-Cl⁻ and H⁺-Ca²⁺-Cl⁻ solutions are not mentioned in Table 5. We set the values of $\theta_{\text{H,c}}$ and $\psi_{\text{H,c,Cl}}$ (where c is Mg²⁺ or Ca²⁺) in the Waters and Millero (2013) model to constant values in this work because of inconsistencies between the equations presented by Waters and Millero in their Table A7 and the data (EMFs, over a range of temperatures) from which they had been derived. It is therefore recommended that these parameters be redetermined as functions of temperature.

Finally, several of the aqueous mixtures discussed above have ions, and therefore parameters, in common. Self-consistency of the parameter set is essential for both the accuracy and reliability of the model, and the suggested improvements will entail other model revisions (e.g., $\theta_{\text{Cl,SO}_4}$ and $\psi_{\text{Cl,SO}_4,\text{Na}}$ determined from data for aqueous NaCl-Na₂SO₄ also occur in the model for H⁺-Na⁺-Cl⁻-HSO₄⁻-SO₄²⁻ solutions). This will be true of the revised model of aqueous H₂SO₄, suggested in section 8.2, which will require redetermination of interaction parameters for all acid sulphate mixtures.

8.4. Uncertainty calculations

In this study we have applied a highly simplified approach in which all interaction parameters are assumed to be determined from a single type of thermodynamic data (osmotic coefficients determined by isopiestic equilibrium) at a single temperature. A more realistic approach should include the following: (i) The use of Harned cell EMFs as a second type of measurement, with its own characteristic random and systematic uncertainties, from which interaction parameter values are obtained. This would improve the uncertainty treatment of the important H⁺-Cl⁻ and H⁺-M²⁺-Cl⁻ interactions, for example. (ii) The use of salt solubilities as a third measurement category, because these have been used to determine many ion-ion mixture parameters in the model. (iii)

Realistically simulating the number, type, and range of molalities of datasets available for each set of interaction parameters, instead of assuming a single isopiestic dataset spanning the same molality range in every case. (iv) The determination of parameter variances and covariances directly (and not by simulation) for the key interactions that contribute the most uncertainty to model outputs, by refitting to original measurements.

The extension of the treatment of Pitzer parameter variances and covariances to other temperatures can partly be addressed by (iv) above, for a small number of individual solutes and mixtures. For the more general case it will be necessary to treat differently parameters that are known only at a single temperature (and for which variances should be expanded if they are used at other temperatures), and those for which there are data from which the variation of the parameters with temperature is known.

9. Summary and conclusions

Here we have implemented the Waters and Millero (2013) and Clegg and Whitfield (1995) chemical speciation models of artificial seawater. The propagation of uncertainties of the interaction parameters and thermodynamic equilibrium constants has been included in the models, for the first time, and a simplified method of estimating their variances and covariances has been developed. This has enabled the estimation of indicative uncertainties in model outputs such as solute activity, speciation, and EMF, and allows the identification of the interaction parameters that contribute most to the overall uncertainty and which should therefore be the subject of future efforts to increase the accuracy of the models.

Comparisons made in sections 5 and 6 show that model calculated EMFs do not yet agree with measured values to within experimental uncertainty for acidified artificial seawater of various salinities. The calculated total uncertainties in modelled EMFs are large enough that the difference between measured and modelled EMFs at 25 °C lies within the uncertainty envelope of the modelled EMFs in most cases (see Figs. 2 and 4). However, this is probably too large given that the variance contribution of H⁺-Cl⁻ interactions is overestimated because of the assumption of osmotic coefficients – rather than EMFs – as the underlying data from which they were determined (section 3.4, and Supporting Information). It is important that the treatment of uncertainties be extended to include EMF measurements as a second data type, as noted above.

Total uncertainties in calculated EMFs, including the standard EMF E^* , are dominated by contributions from $\ln(K(\text{HSO}_4^-))$ and a small number of interaction parameters, mainly those for H⁺-Cl⁻. This knowledge will greatly assist in improving the accuracy of the model and we have recommended additional work to be carried out.

Calculations at two temperatures of the standard EMF, E^* , used in the definition of the total pH scale suggest both that the empirical extrapolation used to determine its values (Dickson, 1990) is satisfactory and that an accurate model of artificial seawater media – one which agrees with measured EMFs to within experimental uncertainty – is attainable.

An extension of the model to include the species Tris and TrisH⁺ is recommended, and is the subject of a companion paper in this journal (Clegg et al., 2022). Such an extension will enable the pH of Tris buffers to be modelled directly, and some of the approximations made in the definition of the total pH scale quantified. These include, for example, the effect of the difference term that arises from the use of E^* (determined in pure artificial seawater) for solutions containing the buffer. An extension will also help extend the total pH scale to lower salinity, develop definitions of pH for natural water compositions other than that of seawater, and carry out conversions between total pH, and free H⁺ ion

concentrations and activities.

Declaration of Competing Interest

None.

Acknowledgements

The work of M.P.H. and S.L.C. was supported by the Natural Environment Research Council of the UK (award NE/P012361/1), and A.G. D. by the U.S. National Science Foundation (award OCE-1744653), both

under the joint NERC/NSF:GEO scheme. The contribution of J.F.W. was supported by the National Institute of Standards and Technology of the U.S.A. This publication is a contribution of SCOR Working Group 145 (SCOR is the Scientific Committee on Oceanic Research) and of the Joint Committee on the Properties of Seawater which is sponsored by SCOR, the International Association for the Properties of Water and Steam, and the International Association for the Physical Sciences of the Oceans. The work of WG 145 presented in this article results, in part, from funding provided by national committees of SCOR and from a grant to SCOR from the U.S. National Science Foundation (OCE-1840868).

Appendix A. Pitzer interaction parameters that are equal to zero

An aqueous solution containing six cations and four anions can potentially require twenty four sets of pure solution cation-anion parameters ($\beta_{ca}^{(0,2)}$ and $C_{ca}^{(0,1)}$), and over one hundred cation-cation-anion and anion-anion-cation parameters. In solutions containing uncharged, neutral, solutes there are further interaction parameters for neutral-neutral, neutral-ion, and neutral-cation-anion-parameters (Pitzer, 1991). However, a large number of parameters are set to zero, and generally fall into the following categories: (i) one or more of the potentially five pure solution ion-ion-interaction parameters for an individual cation-anion pair ($\beta_{ca}^{(0,2)}$, $C_{ca}^{(0,1)}$), which are set to zero because not all of the parameters are required in order to fit the available thermodynamic data for the solute. These zero-valued parameters are not considered to contribute to the overall uncertainty. (ii) Parameters set to zero because the interacting species participate in an equilibrium so that the parameter would be redundant (e.g., θ_{SO_4,HSO_4}). (iii) Parameters set to zero because the species would participate in an acid-base reaction (e.g., $MgOH^+$ and H^+ , or HSO_4^- and OH^-). (iv) Parameters set to zero because there are no data from which to determine their values.

Parameters for cases (ii) and (iii) above do not contribute to the overall uncertainty of a calculation. However, it is possible to address the problem of case (iv) by using literature data for many different solutes to determine average values and standard deviations for interaction parameters of different charge types. These average values can be used to assess the possible influence of the unknown interactions, and their uncertainties, on model-calculated quantities. We have obtained these average values for the principal pure solutions and mixture parameters, and they are listed, with data sources, in Tables A1 and A2. The parameters λ_{nc} , λ_{na} , and ζ_{nca} for interactions involving a neutral solute n are included, although they are not used in this study.

In the treatment of the pure solution parameters we have not included the $C_{ca}^{(0)}$ and $C_{ca}^{(1)}$ parameters, but have recognised the correlation of $\beta_{ca}^{(0)}$ and $\beta_{ca}^{(1)}$ values for 1:1, 2:1, and 1:2 electrolytes (Table A1). The ranges of values of the individual mixture parameters in Table A2 are wide, even though we have excluded from consideration extreme values that involve either very large ions, or small ions which have a high charge density (such as Li^+). Consequently many of the mean values listed in Table A2 differ from zero by less than one standard deviation.

Table A1

Mean values of $\beta^{(0)}$ and $\beta^{(1)}$ interaction parameters for 1:1 and 1:2 electrolytes at 25 °C.

Charge type	$\beta^{(0)}$	Std. Dev. ^a	$\beta^{(1)}$	Std. Dev. ^a	N ^b
1:1	0.0503	0.091	0.1951	0.13	55
2:1 and 1:2	0.243	0.19	1.447	0.40	66
Equation for 1:1 electrolytes					
$\beta^{(1)} = P_1 + P_2 \cdot \beta^{(0)} - P_3 \cdot (\beta^{(0)} + 0.2)^{1.5}$			Covariance Matrix ^c		
P_1	0.477718		0.0158142	0.120858	−0.165664
P_2	4.50697		0.120858	0.954116	−1.28372
P_3	−4.0671		−0.165664	−1.28372	1.75041
Equation for 2:1 and 1:2 electrolytes					
$\beta^{(1)} = Q_1 + Q_2 \cdot \beta^{(0)} - Q_3 \cdot (\beta^{(0)} + 0.2)^{1.5}$			Covariance Matrix ^d		
Q_1	1.16679		0.016572	0.150116	−0.164822
Q_2	6.03467		0.150116	1.68795	−1.76750
Q_3	−4.02018		−0.164822	−1.76750	1.87490

Notes: Values of the two parameters were taken from Pitzer and Mayorga (1973), Table I (1:1 charge type) and Tables VI and VII (2:1 and 1:2 charge types).

^a The standard deviation of the parameter value in the column to the left. For $\beta^{(1)}$ the standard deviation was calculated using the fitted equation and covariance matrix presented in this table.

^b The number of pairs of ($\beta^{(0)}$, $\beta^{(1)}$) fitted.

^c The covariance matrix of the fitted parameters P_{1-3} . The variances of the parameters are the three values on the diagonal (top left to bottom right), and the other values are covariances. (For example, the covariance of P_1 and P_3 is −0.165664.)

^d The covariance matrix of the fitted parameters Q_{1-3} .

Table A2Mean values of θ_{ii} , ψ_{ij} , λ_{ni} , and ζ_{nca} interaction parameters at 25 °C for mixed electrolytes and uncharged solutes.

Parameter	Charge type	Mean ^a	Std. Dev. ^b	Range ^c	N ^d
θ_{cc}	1:1	-0.0119	0.032	-0.097–0.0793	37
θ_{cc}	2:1 and 1:2	0.0597 *	0.031	-0.00535–0.1167	54
θ_{cc}	2:2	0.0121	0.092	-0.1844–0.1722	12
$\psi_{cc'a}$	1:1	-0.00574	0.0070	-0.0215–0.0101	81
$\psi_{cc'a}$	2:1 and 1:2	-0.0151	0.021	-0.056–0.031	91
$\psi_{cc'a}$	2:2	0.00185	0.022	-0.0332–0.0289	13
θ_{aa}	1:1	-0.00607	0.062	-0.09214–0.120	16
θ_{aa}	2:1 and 1:2	0.0210	0.069	-0.105–0.130	18
$\psi_{aa'c}$	1:1	-0.0107	0.026	-0.0960–0.0989	31
$\psi_{aa'c}$	2:1 and 1:2	-0.00859	0.021	-0.060–0.031	39
λ_{nc}	1	0.0463	0.059	-0.070–0.149	35
λ_{nc}	other ^e	0.0228	0.19	-0.311–0.285	35
λ_{nc}	other (O ₂ and CO ₂)	0.196 *	0.079	0.075–0.285	7
λ_{nc}	other (Tris and NH ₃)	-0.121 *	0.10	-0.311–0.021	8
λ_{na}	1	0.00161	0.064	-0.150–0.103	17
λ_{na}	other	0.0776	0.12	-0.164–0.174	9
ζ_{nca}	1:1 ^f	-0.00873	0.012	-0.0281–0.0231	15
ζ_{nca}	other	-0.0149	0.021	-0.046–0.46	17

Notes: Values of the parameters were taken from Kim and Frederick (1988); Pitzer and Kim (1974); Pitzer (1991); Clegg and Whitfield (1995); Clegg and Brimblecombe (1988a, 1988b); Harvie et al. (1984); Waters and Millero (2013); Millero and Pierrot (1998); Møller (1988); Greenberg and Møller (1989); Lach et al. (2018); Spencer et al. (1990); Toner and Catling (2017); Plummer et al. (1988) (including the parameter file of the PHREEQC program); Christov and Møller (2004); Christov (2012); Lassin et al. (2015); Christov (2004); Qafoku and Felmy (2007); Felmy et al. (2000); Nie et al. (2020); Wang et al. (2019); Lach et al. (2017); Gallego-Urrea and Turner (2017); Tishchenko (2000); Lodeiro et al. (2021). Duplicate values were removed from the dataset.

^a Where there were two or more different values for the same interaction parameter (for the same ions) each was given a reduced weight (1/2 in the case of two values, 1/3 in the case of three, etc.). Values of the mean that differ from zero by more than one standard deviation are marked by “*”.

^b The standard deviation.

^c The range of parameter values that were used to determine the mean.

^d The number of values used in the calculation of the mean.

^e Other than unity (ion with a single charge).

^f Both the cation and anion are singly charged.

Appendix B. Calculation of variances of model outputs

This requires, first, a row vector (**J**) of partial derivatives of the model-calculated output with respect to each individual interaction parameter, and natural logarithm of each equilibrium constant ($\ln(K)$). These are determined numerically, as noted in the text. Second, there is a square matrix **C** containing the variances and covariances of all parameters and $\ln(K)$, which is assembled from the values determined as described earlier (and in the same order as the partial derivatives), thus:

$$\mathbf{J} = \left[\frac{\partial y}{\partial p_1} \quad \frac{\partial y}{\partial p_2} \quad \frac{\partial y}{\partial p_3} \quad \dots \quad \frac{\partial y}{\partial p_n} \right] \quad (\text{B.1})$$

where y is the calculated model output for the solution of interest (for example an EMF, mH^+ , or a mean activity coefficient), and $p_{(1-n)}$ are the individual Pitzer model parameters and logarithms of equilibrium constants. The matrix **C** is:

$$\mathbf{C} = \begin{bmatrix} \sigma^2(p_1) & \sigma(p_1, p_2) & \sigma(p_1, p_3) & \dots & \sigma(p_1, p_n) \\ \sigma(p_2, p_1) & \sigma^2(p_2) & \sigma(p_2, p_3) & \dots & \sigma(p_2, p_n) \\ \sigma(p_3, p_1) & \sigma(p_3, p_2) & \sigma^2(p_3) & \dots & \sigma(p_3, p_n) \\ \vdots & \vdots & \vdots & \ddots & \vdots \\ \sigma(p_n, p_1) & \sigma(p_n, p_2) & \sigma(p_n, p_3) & \dots & \sigma^2(p_n) \end{bmatrix} \quad (\text{B.2})$$

where $\sigma^2(p_i)$ is the variance of parameter (or $\ln(K)$) i , and $\sigma(p_i, p_j)$ is the covariance of parameters p_i and p_j . In the Supporting Information the variances and covariances of groups of interaction parameters are presented as individual small matrices (for example a 5×5 matrix for the parameters $\beta_{ca}^{(0)}$, $\beta_{ca}^{(1)}$, $\beta_{ca}^{(2)}$, $C_{ca}^{(0)}$, and $C_{ca}^{(1)}$ for cation c and anion a). To create matrix **C**, all of these small matrices, and the individual variances of each $\ln(K)$, are combined such that: (i) the variances ($\sigma^2(p_i)$) form the diagonal of **C**; (ii) the order of the parameters and $\ln(K)$, both along rows and down columns, is the same as in row vector **J**. All other matrix values are set to zero.

The total variance in the model output y , $\sigma^2(y)$, due to the uncertainties in the interaction parameters and $\ln(K)$, is obtained by two matrix multiplications:

$$\mathbf{D} = \mathbf{J} \bullet \mathbf{C} \quad (\text{B.3})$$

where **D** is a matrix with a single row and n columns, and:

$$\sigma^2(y) = \mathbf{D} \bullet \mathbf{J}^T \quad (\text{B.4})$$

where \mathbf{J}^T is the transpose of **J**. It is also valuable to obtain contributions of individual $\ln(K)$, interaction parameters, and groups of parameters to the total variance and to be able to separate these into both variance contributions and covariance contributions. The individual variance contributions of

each parameter p_i are simplest to obtain, and are given by:

$$\sigma^2(y)(p_i) = (\partial y / \partial p_i)^2 \sigma^2(p_i) \quad (\text{B.5})$$

where $\sigma^2(y)(p_i)$ denotes the contribution of the variance (*not* covariances) of parameter p_i to the total variance of model output y . The covariance contribution of each parameter to the total variance can be determined in the following steps: first, calculate a matrix \mathbf{D}' from the matrix multiplication $\mathbf{J} \bullet \mathbf{C}$ but with all values on the diagonal of \mathbf{C} set to zero. Second, multiply elements i of \mathbf{J} and \mathbf{D}' by each other to obtain the covariance contribution of p_i to the total variance of y .

In cases where results of multiple model simulations are being processed at the same time, values of the partial derivatives of the model output quantity with respect to the parameters and $\ln(K)$ are added as additional rows to \mathbf{J} , one row for each simulation. In the plotted uncertainty profiles presented in this study the variance contributions of groups of parameters have been combined (e.g., each of the sets of pure solution interaction parameters $\beta_{\text{ca}}^{(1-2)}$, $\text{C}_{\text{ca}}^{(0,1)}$). This is done by simple addition of the variance and covariance contributions calculated as described above.

Appendix C. Supplementary data

There are 10 numbered documents of supporting information. The first document summarises the contents of the others, and lists the tables and charts that appear in each one. The subjects covered are: the simulation of uncertainties; values of variances and covariances for interactions and equilibrium constants for HSO_4^- dissociation, and MgOH^+ formation; values of the Pitzer parameters and equilibrium constants for both models; and calculated equilibrium solute molalities and activity coefficients for program verification. Document number four contains an application of the uncertainty simulation method to osmotic and activity coefficients of pure aqueous NaCl and HCl. It is expected that software tools incorporating the model of Waters and Millero (2013), as amended in this work, will be released in late 2022. See website marchemspec.org for future announcements, or contact the corresponding author. Supplementary data to this article can be found online at [<https://doi.org/10.1016/j.marchem.2022.104095>].

References

- Anes, B., Bettencourt Silva, R.J.N., Martins, H.F.P., Oliveira, C.S., Camões, M.F., 2016. Compatibility of activity coefficients estimated experimentally and by Pitzer equations for the assessment of seawater pH. *Accred. Qual. Assur.* 21, 1–7.
- Archer, D.G., 1992. Thermodynamic properties of the NaCl + H₂O system II. Thermodynamic properties of NaCl(aq), NaCl.2H₂O(cr), and phase equilibria. *J. Phys. Chem. Ref. Data* 21, 793–829.
- Archer, D.G., 1999. Thermodynamic properties of the KCl + H₂O system. *J. Phys. Chem. Ref. Data* 28, 1–17.
- Archer, D.G., Carter, R.W., 2000. Thermodynamic properties of the NaCl + H₂O system. 4. Heat capacities of H₂O and NaCl(aq) in cold-stable and supercooled states. *J. Phys. Chem. B* 104, 8563–8584.
- Campbell, D.M., Millero, F.J., Roy, R.N., Roy, L.N., Lawson, M., Vogel, K.M., Porter-Moore, C., 1993. The standard potential for the hydrogen-silver, silver chloride electrode in synthetic seawater. *Mar. Chem.* 44, 221–233.
- Carslaw, K.S., Clegg, S.L., Brimblecombe, P., 1995. A thermodynamic model of the system HCl-HNO₃-H₂SO₄-H₂O, including solubilities of HBr, from <200 K to 328 K. *J. Phys. Chem.* 99, 11557–11574.
- Christov, C., 2004. Pitzer ion-interaction parameters for Fe(II) and Fe(III) in the quinary {Na+K+Mg+Cl+SO₄+H₂O} system at T = 298.15 K. *J. Chem. Thermodyn.* 36, 223–235.
- Christov, C., 2012. Temperature variable chemical model of bromide-sulfate solution interaction parameters and solid-liquid equilibria in the Na-K-Ca-Br-SO₄-H₂O system. *CALPHAD* 36, 71–81.
- Christov, C., Möller, N., 2004. A chemical equilibrium model of solution behaviour and solubility in the H-Na-K-Ca-OH-Cl-HSO₄-SO₄-H₂O system to high concentration and temperature. *Geochim. Cosmochim. Acta* 68, 3717–3739.
- Clarke, E.C.W., Glew, D.N., 1985. Evaluation of the thermodynamic functions for aqueous sodium chloride from equilibrium and calorimetric measurements below 154 °C. *J. Phys. Chem. Ref. Data* 14, 489–610.
- Clegg, S.L., Brimblecombe, P., 1988a. Equilibrium partial pressures of strong acids over concentrated saline solutions. II. HCl. *Atmos. Environ.* 22, 117–129.
- Clegg, S.L., Brimblecombe, P., 1988b. Equilibrium partial pressures of strong acids over concentrated saline solutions. Part I. HNO₃. *Atmos. Environ.* 22, 91–100.
- Clegg, S.L., Humphreys, M.P., Waters, J.F., Turner, D.R., Dickson, A.G., 2022. Chemical speciation models based upon the Pitzer activity coefficient equations, including the propagation of uncertainties. II. Tris buffers in artificial seawater at 25 °C, and an assessment of the seawater 'Total' pH scale. *Marine Chemistry* 104096.
- Clegg, S.L., Whitfield, M., 1991. Activity coefficients in natural waters. In: Pitzer, K.S. (Ed.), *Activity Coefficients in Electrolyte Solutions*, 2nd edn. CRC Press, Boca Raton, pp. 279–434.
- Clegg, S.L., Whitfield, M., 1995. A chemical model of seawater including dissolved ammonia, and the stoichiometric dissociation constant of ammonia in estuarine water and seawater from −2 ° to 40 °C. *Geochim. Cosmochim. Acta* 59, 2403–2421.
- Clegg, S.L., Rard, J.A., Pitzer, K.S., 1994. Thermodynamic properties of 0–6 mol kg^{−1} aqueous sulphuric acid from 273.15 to 328.15 K. *J. Chem. Soc. Faraday Trans. 90*, 1875–1894.
- DelValls, T.A., Dickson, A.G., 1998. The pH of buffers based on 2-amino-2-hydroxymethyl-1,3-propanediol ("tris") in synthetic sea water. *Deep-Sea Res.* I 45, 1541–1554.
- Dickson, A.G., 1990. Standard potential of the (Ag(s) + 1/2H₂(g) = Ag(s) + HCl(aq)) cell and the dissociation constant of bisulphate ion in synthetic seawater from 273.15 to 318.15 K. *J. Chem. Thermodynamics* 22, 113–127.
- Dickson, A.G., Wesolowski, D.J., Palmer, D.A., Mesmer, R.E., 1990. Dissociation constant of bisulphate ion in aqueous sodium chloride solutions to 250 °C. *J. Phys. Chem.* 94, 7978–7985.
- Dickson, A.G., Camões, M.F., Spitzer, P., Fiescaro, P., Stoica, D., Pawlowicz, R., Feistel, R., 2016. Metrological challenges for measurements of key climatological observables. Part 3: Seawater. *Metrologia* 53, R26–R39.
- Felmy, A.R., Onishi, L.M., Foster, N.S., Rustad, J.R., Rai, D., Mason, M.J., 2000. An aqueous thermodynamic model for the Pb²⁺-Na⁺-K⁺-Ca²⁺-Mg²⁺-H⁺-Cl[−]-SO₄^{2−}-H₂O system to high concentration: Application to WIPP brines. *Geochim. Cosmochim. Acta* 64, 3615–3628.
- Friese, E., Ebel, A., 2010. Temperature dependent thermodynamic model of the system H⁺-NH₄⁺-Na⁺-SO₄^{2−}-NO₃[−]-Cl[−]-H₂O. *J. Phys. Chem. A* 114, 11595–11631.
- Gallego-Urrea, J.A., Turner, D.R., 2017. Determination of pH in estuarine and brackish waters: Pitzer parameters for Tris buffers and dissociation constants for m-cresol purple at 298.15 K. *Mar. Chem.* 195, 84–89.
- Gibbard, H.F., Scatchard, G., Rousseau, R.A., Creek, J.L., 1974. Liquid-vapor equilibrium of aqueous sodium chloride, from 298 to 373 K and from 1 to 6 mol kg^{−1}, and related properties. *J. Chem. Eng. Data* 19 (3), 281–288.
- Gordon, A.R., 1943. Isopiestic measurements in dilute solutions; the system potassium chloride-sodium chloride at 25° at concentrations from 0.03 to 0.10 molal. *J. Am. Chem. Soc.* 65, 221–224.
- Greenberg, J.P., Möller, N., 1989. The prediction of mineral solubilities in natural waters: a chemical equilibrium model for the Na-K-Ca-Cl-SO₄-H₂O system to high concentration from 0 to 250 °C. *Geochim. Cosmochim. Acta* 53, 2503–2518.
- Hamer, W.J., Wu, Y.C., 1972. Osmotic coefficients and mean activity coefficients of uni-univalent electrolytes in water at 25 °C. *J. Phys. Chem. Ref. Data* 1, 1047–1099.
- Hansson, I., 1973. A new set of pH-scales and standard buffers for sea water. *Deep-Sea Res.* 20, 479–491.
- Harned, H.S., 1959. The thermodynamic properties of the system: hydrochloric acid, sodium chloride and water from 0 to 50°. *J. Phys. Chem.* 63, 1299–1302.
- Harned, H.S., Sturgis, R.D., 1925. The free energy of sulphuric acid in aqueous sulphate solutions. *J. Amer. Chem. Soc.* 47, 945–953.
- Harvie, C.E., Weare, J.H., 1980. The prediction of mineral solubilities in natural waters: the Na-K-Mg-Ca-Cl-SO₄-H₂O systems from zero to high concentration at 25 °C. *Geochim. Cosmochim. Acta* 44, 981–997.
- Harvie, C.E., Möller, N., Weare, J.H., 1984. The prediction of mineral solubilities in natural waters: the Na-K-Mg-Ca-H-Cl-SO₄-OH-HCO₃-CO₃-CO₂-H₂O system to high ionic strengths at 25 °C. *Geochim. Cosmochim. Acta* 48, 723–751.
- Hawkins, J.E., 1932. The activity coefficients of hydrochloric acid in uni-univalent chloride solutions at constant total molality. *J. Am. Chem. Soc.* 54, 4480–4487.
- Holmes, H.F., Mesmer, R.E., 1986. Thermodynamics of aqueous solutions of the alkali metal sulphates. *J. Soln. Chem.* 15, 495–518.
- Holmes, H.F., Busey, R.H., Simonson, J.M., Mesmer, R.E., Archer, D.G., Wood, R.H., 1987. The enthalpy of dilution of HCl(aq) to 648 K and 40 MPa. *Thermodynamic properties. J. Chem. Thermo.* 19, 863–890.
- Hovey, J.K., Hepler, L.G., 1990. Thermodynamics of sulphuric acid: apparent and partial molar heat capacities and volumes of aqueous HSO₄[−] from 0–55 °C and calculation of the second dissociation constant to 350 °C. *J. Chem. Soc. Faraday Trans.* 86, 2831–2839.

- Hovey, J.K., Pitzer, K.S., Rard, J.A., 1993. Thermodynamics of $\text{Na}_2\text{SO}_4(\text{aq})$ at temperatures T from 273 K to 373 K and of $\{(1-y)\text{H}_2\text{SO}_4 + y\text{Na}_2\text{SO}_4\}(\text{aq})$ at $T = 298.15$ K. *J. Chem. Thermo.* 25, 173–192.
- Janis, A.A., Ferguson, J., 1939. Sodium chloride solutions as an isopiestic standard. *Can. J. Res.* 17b, 215–230.
- Kho, K.H., Ramette, R.W., Culberson, C.H., Bates, R.G., 1977. Determination of hydrogen ion concentrations in seawater from 5 to 40 °C: standard potentials at salinities from 20 to 45 ppt salinity. *Anal. Chem.* 49, 29–34.
- Kim, H.T., Frederick, W.J., 1988. Evaluation of Pitzer ion interaction parameters of aqueous mixed electrolyte solutions at 25 °C. 2. Ternary mixing parameters. *J. Chem. Eng. Data* 33, 278–283.
- Kirgintsev, A.N., Lukyanov, A.V., 1967. Isopiestic study of sodium chloride - potassium chloride - calcium chloride - water solutions at 25 °C. *Russ. J. Phys. Chem.* 41, 54.
- Knopf, D.A., Luo, B.P., Krieger, U.K., Koop, T., 2003. Thermodynamic dissociation constant of the bisulfate ion from Raman and ion interaction modeling studies of aqueous sulfuric acid at low temperatures. *J. Phys. Chem. A* 107, 4322–4332.
- Lach, A., Andre, L., Lassin, A., 2017. Darapskite solubility in basic solutions at 25 °C: A Pitzer model for the $\text{Na-NO}_3\text{-SO}_4\text{-OH-H}_2\text{O}$ system. *Appl. Geochem.* 78, 311–320.
- Lach, A., André, L., Guignot, S., Christov, C., Henocq, P., Lassin, A., 2018. A Pitzer parametrization to predict solution properties and salt solubility in the $\text{H-Na-K-Ca-Mg-NO}_3\text{-H}_2\text{O}$ system at 298.15 K. *J. Chem. Eng. Data* 63, 787–800.
- Lassin, A., Christov, C., Andre, L., Azaroual, M., 2015. A thermodynamic model of aqueous electrolyte solution behavior and solid-liquid equilibrium in the $\text{Li-H-Na-K-Cl-OH-H}_2\text{O}$ system to very high concentrations (40 molal) and from 0 to 250 °C. *Am. J. Sci.* 315, 204–256.
- Lietzke, M.H., Stoughton, R.W., Young, T.F., 1961. The bisulphate acid constant from 25 to 225° as computed from solubility data. *J. Phys. Chem.* 65, 2247–2249.
- Lodeiro, P., Turner, D.R., Achterberg, E.P., Gregson, F.K.A., Reid, J.P., Clegg, S.L., 2021. Solid-liquid equilibria in aqueous solutions of Tris, Tris-NaCl , Tris-TrisHCl , and $\text{Tris-(TrisH)}_2\text{SO}_4$ at temperatures from 5 to 45 °C. *J. Chem. Eng. Data* 66 (437–455).
- Lu, X.-M., Wang, Q.-P., Zhao, G.-Z., Chen, S.-S., Lu, D.-Z., 2005. Harned's rule of HCl in magnesium sulfate solutions. *Acta Phys.-Chim. Sin.* 21 (12), 1384–1389.
- Macaskill, J.B., Robinson, R.A., Bates, R.G., 1977. Activity coefficient of hydrochloric acid in aqueous solutions of sodium chloride. *J. Soln. Chem.* 6, 385–392.
- Marshall, W.L., Jones, E.V., 1966. Second dissociation constant of sulfuric acid from 25 to 350° evaluated from solubilities of calcium sulfate in sulfuric acid solutions. *J. Phys. Chem.* 70, 4028–4040.
- Matsushima, Y., Okuwaki, A., 1988. The second dissociation constant of sulphuric acid at elevated temperatures from potentiometric measurements. *Bull. Chem. Soc. Jpn.* 61, 3344–3346.
- Meinrath, G., 2002. Extended traceability of pH: an evaluation of the role of Pitzer's equations. *Anal. Bioanal. Chem.* 374, 796–805.
- Millero, F.J., Pierrot, D., 1998. A chemical equilibrium model for natural waters. *Aquat. Geochem.* 4, 153–199.
- Møller, N., 1988. The prediction of mineral solubilities in natural waters: a chemical equilibrium model for the $\text{Na-Ca-Cl-SO}_4\text{-H}_2\text{O}$ system, to high temperature and concentration. *Geochim. Cosmochim. Acta* 52, 821–837.
- Mussini, P.R., Longhi, P., Mussini, T., Rondinini, S., 1989. The second ionization constant of aqueous sulphuric acid at 298.15 K from the electromotive force of the unbuffered cell: $\text{H}_2\text{S(g)}, \text{H}_2\text{SO}_4(\text{aq}), \text{Hg}_2\text{SO}_4(\text{s}), \text{Hg}$. *J. Chem. Thermo.* 21, 625–629.
- Nair, V.S.K., Nancollas, G.H., 1958. Thermodynamics of ion association. Part V. Dissociation of the bisulfate ion. *J. Chem. Soc.*, 4144–4147.
- Nie, G.-L., Sang, S.-H., Cui, R.-Z., Wu, Z.-Z., Ye, C., Gao, Y.-Y., 2020. Measurements and calculations of solid-liquid equilibria in two quaternary systems: $\text{LiCl-NaCl-SrCl}_2\text{-H}_2\text{O}$ and $\text{LiCl-KCl-SrCl}_2\text{-H}_2\text{O}$ at 298 K. *Fluid Phase Equilib.* 509, Art. 112458, 10 pp.
- Orr, J.C., Epitalon, J.-M., Dickson, A.G., Gattuso, J.-P., 2018. Routine uncertainty propagation for the marine carbon dioxide system. *Mar. Chem.* 207, 84–107.
- Partanen, J.I., Juusola, P.M., Vahteristo, K.P., de Mendonça, A.J.G., 2007. Re-evaluation of the activity coefficients of aqueous hydrochloric acid solutions up to a molality of 16.0 mol·kg⁻¹ using the Hückel and Pitzer Equations at temperatures from 0 to 50 °C. *J. Solut. Chem.* 36, 39–59.
- Pierrot, D., Millero, F.J., 2016. The speciation of metals in natural waters. *Aquat. Geochem.* 23 (1), 1–20.
- Pierrot, D., Millero, F.J., Roy, L.N., Roy, R.N., Doneski, A., Niederschmidt, J., 1997. The activity coefficients of HCl in $\text{HCl-Na}_2\text{SO}_4$ solutions from 0 to 50 °C and ionic strengths up to 6 molal. *J. Solut. Chem.* 26, 31–45.
- Pitzer, K.S., 1991. Ion interaction approach: theory and data correlation. In: Pitzer, K.S. (Ed.), *Activity Coefficients in Electrolyte Solutions*, 2nd edn. CRC Press, Boca Raton, pp. 75–153.
- Pitzer, K.S., Kim, J., 1974. Thermodynamics of electrolytes IV: activity and osmotic coefficients of mixed electrolytes. *J. Am. Chem. Soc.* 96, 5701–5707.
- Pitzer, K.S., Mayorga, G., 1973. Thermodynamics of electrolytes II: activity and osmotic coefficients for strong electrolytes with one or both ions univalent. *J. Phys. Chem.* 77, 2300–2308.
- Pitzer, K.S., Roy, R.N., Silvester, L.F., 1977. Thermodynamics of electrolytes 7. Sulphuric acid. *J. Am. Chem. Soc.* 99, 4930–4936.
- Plummer, L.N., Parkhurst, D.L., Fleming, G.W., Dunkle, S.A., 1988. A Computer Program Incorporating Pitzer's Equations for Calculation of Geochemical Reactions in Brines. In: *Water-Resources Investigations Report 88-4153*. U.S. Geological Survey, Reston, VA.
- Qafoku, O., Felmy, A.R., 2007. Development of accurate chemical equilibrium models for oxalate species to high ionic strength in the system: $\text{Na-Ba-Ca-Mn-Sr-Cl-NO}_3\text{-PO}_4\text{-SO}_4\text{-H}_2\text{O}$ at 25 °C. *J. Solut. Chem.* 36, 81–95.
- Rard, J.A., 1989. Isopiestic determination of the osmotic and activity coefficients of $\{(1-y)\text{H}_2\text{SO}_4 + y\text{Na}_2\text{SO}_4\}(\text{aq})$ at 298.15 K. I Results for $y=0.5$ (NaHSO_4) and $y=0.55595$, 0.70189, and 0.84920. *J. Chem. Thermo.* 21, 539–560.
- Rard, J.A., 1992. Isopiestic determination of the osmotic and activity coefficients of $[(1-y)\text{H}_2\text{SO}_4 + y\text{Na}_2\text{SO}_4](\text{aq})$ at 298.15 K. II Results for $(y=0.12471, 0.24962 \text{ and } 0.37439)$. *J. Chem. Thermo.* 24, 45–66.
- Rard, J.A., Clegg, S.L., 1995. A review of some aspects of electromotive force measurements for the cells: $\text{Pt}[\text{H}_2(\text{g}, p^0)]\text{H}_2\text{SO}_4(\text{aq})|\text{PbO}_2(\text{s})|\text{PbSO}_4(\text{s})|\text{Pt}$, and $\text{Pt}[\text{H}_2(\text{g}, p^0)]\text{H}_2\text{SO}_4(\text{aq})|\text{Hg}_2\text{SO}_4(\text{s})|\text{Hg}(\text{l})|\text{Pt}$, with $p^0 = 0.1$ MPa. *J. Chem. Thermo.* 27, 69–98.
- Rard, J.A., Clegg, S.L., 1999. Isopiestic determination of the osmotic and activity coefficients of $\{z\text{H}_2\text{SO}_4 + (1-z)\text{MgSO}_4\}(\text{aq})$ at $T = 298.15$ K. II. Results for $z = (0.43040, 0.28758, \text{ and } 0.14399)$ and analysis with Pitzer's model. *J. Chem. Thermo.* 31, 399–429.
- Rard, J.A., Platford, R.F., 1991. Experimental methods: isopiestic. In: Pitzer, K.S. (Ed.), *Activity Coefficients in Electrolyte Solutions*, 2nd edn. CRC Press, Boca Raton, pp. 209–277.
- Rard, J.A., Clegg, S.L., Palmer, D.A., 2000. Isopiestic determination of the osmotic coefficients of $\text{Na}_2\text{SO}_4(\text{aq})$ at 25 and 50 degrees C, and representation with ion-interaction (Pitzer) and mole fraction thermodynamic models. *J. Solut. Chem.* 29, 1–49.
- Rard, J.A., Clegg, S.L., Platford, R.F., 2003. Thermodynamics of $\{z\text{NaCl} + (1-z)\text{Na}_2\text{SO}_4\}(\text{aq})$ from $T = 278.15$ K to $T = 318.15$ K, and representation with an extended ion-interaction (Pitzer) model. *J. Chem. Thermo.* 35, 967–1008.
- Reardon, E.J., Beckie, R.D., 1987. Modelling chemical equilibria of acid mine-drainage: the $\text{FeSO}_4\text{-H}_2\text{SO}_4\text{-H}_2\text{O}$ system. *Geochim. Cosmochim. Acta* 51, 2355–2368.
- Robinson, R.A., 1945. The vapour pressures of solutions of potassium chloride and sodium chloride. *Trans. Roy. Soc. NZ* 75, 203–217.
- Robinson, R.A., Sinclair, D.A., 1934. The activity coefficients of the alkali chlorides and of lithium iodide in aqueous solution from vapor pressure measurements. *J. Am. Chem. Soc.* 56, 1830–1835.
- Robinson, R.A., Stokes, R.H., 1970. *Electrolyte Solutions*, 2nd edn. (Revised). Butterworths, London.
- Scatchard, G., Hamer, W.J., Wood, S.E., 1938. Isotonic solutions. I. The chemical potential of water in aqueous solutions of sodium chloride, potassium chloride, sulphuric acid, sucrose, urea and glycerol at 25 °C. *J. Am. Chem. Soc.* 60, 3061–3070.
- Sippola, H., 2013. Critical evaluation of the second dissociation constants for aqueous sulfuric acid over a wide temperature range. *J. Chem. Eng. Data* 58, 3009–3032.
- Sippola, H., Taskinen, P., 2014. Thermodynamic properties of aqueous sulfuric acid. *J. Chem. Eng. Data* 59, 2389–2407.
- Spencer, R.J., Møller, N., Weare, J.H., 1990. The prediction of mineral solubilities in natural waters. A chemical equilibrium model for the $\text{Na-K-Ca-Mg-Cl-SO}_4\text{-H}_2\text{O}$ system at temperatures below 25 °C. *Geochim. Cosmochim. Acta* 54, 575–590.
- Spitzer, P., Fiescaro, P., Meinrath, G., Stoica, D., 2011. pH buffer assessment and Pitzer's equations. *Accred. Qual. Assur.* 16, 191–198.
- Storokin, A.V., Shul'ts, M.M., Langunov, M.D., Okatov, M.A., 1967. Aqueous solutions of strong electrolytes IV. Activity of hydrogen chloride in the hydrochloric acid-sulphuric acid-water system and of sodium chloride in the sodium chloride-sodium sulphate-water system. *Russ. J. Phys. Chem.* 41, 541–543.
- Tishchenko, P.Y., 2000. Non-ideal properties of the $\text{TRIS-TRIS.HCl-NaCl-H}_2\text{O}$ buffer system in the 0–40 °C temperature interval. Application of the Pitzer equations. *Russ. Chem. Bull.* 49 (4), 674–679.
- Toner, J.D., Catling, D.C., 2017. A low-temperature aqueous thermodynamic model for the $\text{Na-K-Ca-Mg-Cl-SO}_4$ system incorporating new experimental heat capacities in Na_2SO_4 , K_2SO_4 , and MgSO_4 solutions. *J. Chem. Eng. Data* 62, 3151–3168.
- Wang, L., Zhang, W., Yang, B., Cai, Y., Yi, J., 2019. Solubility measurements in $\text{Na-F-CO}_3\text{-HCO}_3\text{-H}_2\text{O}$ system at (308.15 and 323.15) K and development of a Pitzer-based equilibrium model for the $\text{Na-F-Cl-SO}_4\text{-CO}_3\text{-HCO}_3\text{-H}_2\text{O}$ system. *J. Chem. Thermo.* 131, 88–96.
- Waters, J.F., Millero, F.J., 2013. The free proton concentration scale for seawater pH. *Mar. Chem.* 149, 8–22.
- Waters, J.F., Millero, F.J., Woosley, R.J., 2014. Corrigendum to "The free proton concentration scale for seawater pH", [MARCH: 149 (2013) 8–22]. *Mar. Chem.* 165, 66–67.
- White, D.R., Robinson, R.A., Bates, R.G., 1980. Activity coefficient of hydrochloric acid in HCl/MgCl_2 mixtures and HCl/NaCl/MgCl_2 mixtures from 5 to 45 °C. *J. Soln. Chem.* 9, 457–465.
- Wu, Y.C., Rush, R.M., Scatchard, G., 1968. Osmotic and activity coefficients for binary mixtures of sodium chloride, sodium sulphate, magnesium sulphate and magnesium chloride in water 25 °C. I. Isopiestic measurements on the four systems with common ions. *J. Phys. Chem.* 72, 4048–4053.
- Young, T.F., Singletary, C.R., Klotz, I.M., 1978. Ionization constants and heats of ionization of the bisulphate ion from 5 to 55 °C. *J. Phys. Chem.* 82, 671–674.